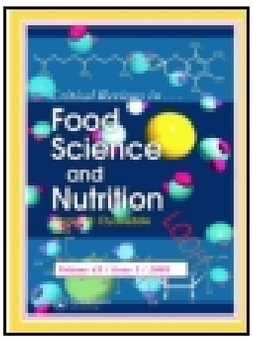

Critical Reviews in Food Science and Nutrition

ISSN: 1040-8398 (Print) 1549-7852 (Online) Journal homepage: http://www.tandfonline.com/loi/bfsn20

Recent advances in rapid and nondestructive determination of fat content and fatty acids composition of muscle foods

Feifei Tao & Michael Ngadi

To cite this article: Feifei Tao & Michael Ngadi (2017): Recent advances in rapid and nondestructive determination of fat content and fatty acids composition of muscle foods, Critical Reviews in Food Science and Nutrition, DOI: 10.1080/10408398.2016.1261332

To link to this article: https://doi.org/10.1080/10408398.2016.1261332

Accepted author version posted online: 24 Jan 2017.
Published online: 05 Jul 2017.

CRITICAL REVIEWS IN FOOD SCIENCE AND NUTRITION
https://doi.org/10.1080/10408398.2016.1261332

Recent advances in rapid and nondestructive determination of fat content and fatty acids composition of muscle foods

Feifei Tao and Michael Ngadi

Department of Bioresource Engineering, McGill University, Ste-Anne-de-Bellevue, Quebec, Canada

ABSTRACT

Conventional methods for determining fat content and fatty acids (FAs) composition are generally based on the solvent extraction and gas chromatography techniques, respectively, which are time consuming, laborious, destructive to samples and require use of hazard solvents. These disadvantages make them impossible for large-scale detection or being applied to the production line of meat factories. In this context, the great necessity of developing rapid and nondestructive techniques for fat and FAs analyses has been highlighted. Measurement techniques based on near-infrared spectroscopy, Raman spectroscopy, nuclear magnetic resonance and hyperspectral imaging have provided interesting and promising results for fat and FAs prediction in varieties of foods. Thus, the goal of this article is to give an overview of the current research progress in application of the four important techniques for fat and FAs analyses of muscle foods, which consist of pork, beef, lamb, chicken meat, fish and fish oil. The measurement techniques are described in terms of their working principles, features, and application advantages. Research advances for these techniques for specific food are summarized in detail and the factors influencing their modeling results are discussed. Perspectives on the current situation, future trends and challenges associated with the measurement techniques are also discussed.

KEYWORDS

Fat; fatty acid; near-infrared spectroscopy; Raman spectroscopy; nuclear magnetic resonance; hyperspectral imaging

Introduction

Fat and fatty acids (FAs) are vital nutritional components of various kinds of foods, as they are important for energetic, metabolic, and structural activities of human beings. In particular, the essential fatty acids (EFAs), or their metabolic derivatives are required for normal growth and physiological integrity and cannot be synthesized in adequate amounts by the human body. The linoleic acid (LA, C18:2 *n*-6) and α-linolenic acid (ALA, C18:3 *n*-3) are now known to be the EFAs for humans. Derivatives such as arachidonic acid (ARA, C20:4 *n*-6), eicosapentaenoic acid (EPA) (C20:5 *n*-3), and docosahexaenoic acid (DHA) (C22:6 *n*-3) are called "conditionally essential" in circumstances such as those which exist in premature infants where they cannot be synthesized by the body in adequate amounts. Moreover, the ALA has also been demonstrated to have health benefits by lowering blood lipid concentrations and reducing the risk of platelet aggregation and thrombosis (Vanschoonbeek et al., 2003). Therefore, adequate amounts of dietary fat/FAs, especially some particular types are essential for our health. In addition, from the viewpoint of food factories, proper amounts of fat content and FAs composition are important for high-quality food. For instance, the fat in meat makes a significant contribution not only to the texture and juiciness but also to the taste and smell of the final product (Fernandez et al., 1999a; Wood et al., 1999). However, some types of fat and FAs are also known to have negative effect on human health (Wood et al., 2008). Reports have shown that an excess in consumption of saturated FAs (SFAs) as well as of some *trans*- and *n*-6 FAs has been associated with negative effects on cholesterolemia, obesity, metabolic syndrome, and coronary heart diseases (Hayes and Khosla, 1992; Hu et al., 1999; Kratz et al., 2013; Shingfield et al., 2008; Stark et al., 2008). In this context, the demand by consumers for information on fat content and FAs composition in foods is growing, and thus it has increasingly become important for food manufacturers to characterize the chemical composition and to provide labeling of chemical composition information in their products.

At present, the conventional methods for determination of fat content and FAs composition in foods are generally based on the solvent extraction and gas chromatography (GC) techniques, respectively. However, these methods are time consuming, laborious, and destructive to the tested samples. They use hazard solvents, also need experienced and properly trained personnel to perform, making them impossible for large-scale detection or integration in an online production in food factories. Therefore, development of innovative and nondestructive detection techniques to facilitate simple, fast, and accurate determination of fat content and FAs composition in muscle foods are attracting increasing attention in the meat industries. Among current emerging technologies, the optical-based methods have been reported to show the greatest potential for online applications (Shackelford et al., 1999; Vote et al., 2003). The use of such

CONTACT Michael Ngadi michael.ngadi@mcgill.ca Department of Bioresource Engineering, McGill University, 21,111 Lakeshore Road, Ste-Anne-de-Bellevue, QC H9×3V9, Canada.

Color versions of one or more of the figures in the article can be found online at www.tandfonline.com/bfsn.

methods has been recently studied extensively and implemented as alternatives to conventional analytical methods for determination of fat content and FAs composition in muscle foods. Therefore, the main goal of this article is to give an overview of the current research progress in application of near-infrared spectroscopy (NIRS), Raman spectroscopy (RS), nuclear magnetic resonance (NMR) and hyperspectral imaging (HSI) techniques to fat and FAs analyses in muscle foods, which consist of pork, beef, lamb, chicken meat, fish, and fish oil. These techniques are described in terms of their working principles, features, and application advantages in fat and FAs analyses. The research advances of each technique in fat and FAs analyses of each specific variety of muscle food are summarized in detail and the factors influencing their modeling results are discussed in this article. In addition, perspectives on their current situation, future trends and challenges are also discussed.

Detection techniques

Near-infrared spectroscopy

Near-infrared region (NIR) in the electromagnetic spectrum is defined to be from 780 to 2526 nm (12821–3959 cm^{-1}) by the American Society of Testing and Materials. This region is located between the red band of the visible light and the mid-infrared regions (Burns and Ciurczak, 2001). NIRS is a rapid and nondestructive technique based on the principle that different chemical bonds absorb or emit different wavelengths of light when the sample is irradiated by continuous changing frequency of NIR light. The absorption intensity is related to the content of the chemical substances in the tested sample (Cen and He, 2007; Prevolnik et al., 2004). The record of NIR region of the electromagnetic spectrum involves the response of the molecular bonds C-H, O-H, N-H, and C-O. These bonds are subject to vibrational energy changes when irradiated by NIR light, and two vibration patterns exist in these bonds including stretch vibration and bent vibration. However, NIR spectra are complex due to highly overlapping and weak absorption bands associated with overtones and combinations of vibrational bonds, which therefore needs the chemometric assistance for spectral interpretation and analysis.

For NIRS, there are three main modes of data collection (Wu and Sun, 2013), namely, reflectance, transmittance, and interactance. The determination of a suitable measurement mode relies on the type of sample and the constituents to be tested. In reflectance mode, the radiation reflected from the sample surface and the detector is located at the same side of the light source to capture the reflected light from the sample, which is usually used for solid or granular samples. Tests in transmittance mode measure the amount of light transmitted through the sample, which is usually small but may carry more valuable information in it (Schaare and Fraser, 2000). In transmittance mode, the detector is located at the opposite side of the illumination, and such a mode is normally used for the analysis of liquid samples and certain solid samples, such as milk, meat, and so on. Interactance mode is a combination of reflectance and transmittance, in which the light source and the detector are positioned parallel to each other on the same side of the tested product (Nicolai et al., 2007). Generally, in the area of food analysis, the measurement modes of reflectance and transmittance are employed for NIRS.

Nowadays, with the development of chemometrics and computer technique, NIRS has been extensively studied as an effective tool for the evaluation of food quality and safety. It can offer a number of important advantages over conventional methods such as rapid and nondestructive measurements, simple or no sample preparation, suitability for online use and simultaneous determination of multiple attributes. The capability of using NIRS technique to predict fat content and FAs composition in foods is due to the absorption of light by the C-H bonds of FAs in the wavelengths of 1100–1400, 1700, and 2200–2400 nm (Williams and Norris, 1987). Moreover, the structure of FAs in foods can also be appreciated in special spectral characteristics and they are, therefore, very accessible for detection by NIRS. The absorptions at 1680, 2150, and 2190 nm are reported to be attributed to the -CH bond joined to a *cis*-unsaturation (Murray and Williams, 1987; Sato et al., 1991). The absorption bands between 2100 and 2200 nm are considered to be related to the length of the chain and the double *cis*- bond, respectively (Sato et al., 1991). As the visible (Vis) spectral range is commonly covered by the NIRS instrument, the following applications of NIRS to fat content and FAs composition analyses are reviewed including the Vis range.

Raman spectroscopy

The phenomenon of inelastic light scattering is known as Raman radiation and was first documented by Raman and Krishnan (1928). When a substance is irradiated with monochromatic light, most of the scattered energy comprises radiation of the incident frequency (Rayleigh scattering). In addition, a very small quantity (0.0001%) of photons with shifted frequency is observed, and is called Raman scattering. There are two types of Raman scattering, namely, Stokes scattering and anti-Stokes scattering. The fraction of photons scattered from molecular centers with less energy than they had before the interaction is called Stokes scattering. The anti-Stokes photons have greater energy than those of the exciting radiation (Fig. 1).

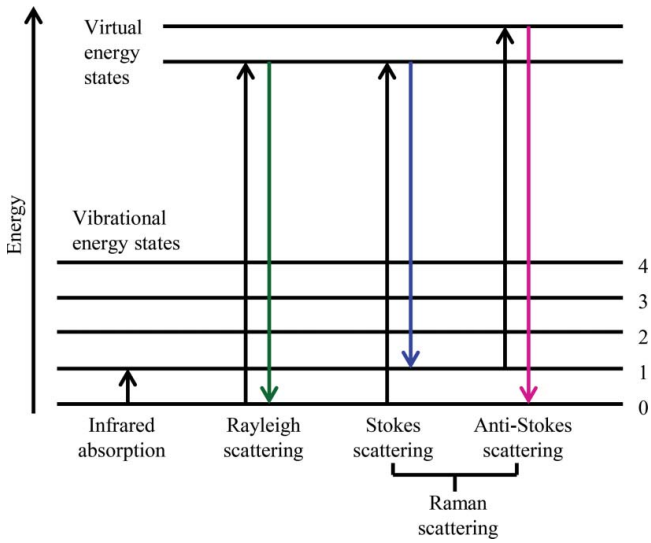

Figure 1. Schematic representation of energy transitions in Raman spectroscopy.

The above-mentioned discovery of Raman scattering gradually paved the way for present-day applications of RS for determining the compositions of samples tested. Raman and infrared (IR) spectroscopy are complementary techniques as both spectra are concerned with measuring associated molecular vibration and rotational energy changes. However, the requirement for vibrational activity in Raman spectra is not a change in dipole moment, as it is in IR spectra, but a change in the polarizability of the molecule. Hence, nonpolar groups such as C=C, C—C, and S—S have intense Raman bands, other than the polar groups such as C=O, N—H, and O—H which have strong IR stretching vibrations. Moreover, Raman scattering is a relatively weak phenomenon that occurs only once in every 10^6–10^8 photons, which are scattered (Smith and Dent, 2005).

RS typically makes use of lasers in the Vis, NIR, or near ultraviolet range for excitation. The interference from strong and broad fluorescence signals of samples combined with low sensitivity have traditionally been some of the major challenges to RS technique However, significant instrumental improvements on stability, sensitivity, and sampling techniques have been achieved, making it possible for an increased number of studies related to RS for food analysis in recent years (Beattie et al., 2004; Wold et al., 2004). A number of technological advances such as holographic notch filters for rejection of elastically scattered light and the availability of long wavelength (750–1064 nm) excitation lasers (which reduce background fluorescence problems) are making the technique more accessible than ever before. For compositional analysis of various foods, RS has an advantage over other optical methods in that the influence of water on the Raman spectra is almost negligible.

The potential of RS for the analysis of fats and FAs in foods has been recognized for some decades. FAs and their degree of saturation can influence the intensity and location of bands in their Raman spectra (Baeten et al., 1996; Li-Chan, 1996; Ozaki et al., 1992). Raman bands observed in fats and oils near 1750, 1660, 1470, 1443, 1306, and 1269 cm^{-1} are assigned undoubtedly to the C=O stretching modes, C=C stretching modes, CH_2 scissoring modes, CH_2 twisting modes, and CH in plane deformation modes. The frequencies of the C=C stretching bands of unsaturated FAs (UFAs) are very sensitive to the configuration around the C=C bond. Thus *trans* and *cis* UFAs give the C=C stretching band in the 1670–1680 and 1650–1665 cm^{-1} regions, respectively. It has been demonstrated that the iodine value (IV), which is a number widely used to indicate the unsaturation level of fat-containing food products, can be estimated directly by measuring the Raman spectra of the food. In particular, it has been noted that oils with high IVs provide an intense C=C stretching band (1660 cm^{-1}). Some authors have also suggested that a comparison in the 1500–1700 cm^{-1} region gives a practical guide for the examination of the unsaturation level of fat-containing food products (Li-Chan, 1996; Ozaki et al., 1992).

Nuclear magnetic resonance

The physical basis of NMR, a spectroscopic technique based on the fact that certain atomic nuclei possess an angular magnetic moment, was first described by the groups of Bloch (Bloch et al., 1946) and Purcell (Purcell et al., 1946), for which they were awarded the 1952 Nobel Prize. The most commonly measured nuclei are ^1H and ^{13}C, although nuclei from the isotopes of many other elements can be observed (^{23}Na, ^{31}P, etc.). All nuclei are electrically charged, therefore, when an external magnetic field is applied, two spin states exist. NMR aligns magnetic moments with an applied constant magnetic field and disturbs this alignment using an orthogonal alternating radio frequency magnetic field. This disturbance induces a resonant phenomenon, which is used in NMR measurements. The signal obtained can be measured in many ways and then processed to generate an NMR spectrum for analysis use.

NMR technique was initially used in the late 1940s to elucidate the structure of molecules in organic chemistry (Gutowsky et al., 1949). However the diverse applications of NMR technique in food science were delayed until the 1980s, primarily due to lack of scientific expertise, high cost of equipment and the absence of NMR parts designed specifically for food purposes (Marcone et al., 2013), although pulsed NMR had been applied to foods earlier. Nowadays, NMR technique has been studied for fat and FA analysis in a wide range of food matrices without destroying the sample or producing hazardous wastes. At present, there are two main types of NMR instrument widely applied to food analysis: (i) low-field nuclear magnetic resonance (LF-NMR) (also called time-domain NMR) and (ii) spectroscopic NMR (signal versus frequency). LF-NMR represents a simplified and cheaper version of a traditional NMR instrument and operates in the frequency range of 2–25 MHz (Aursand et al., 2006). LF-NMR can provide important information about relaxation and diffusion behavior and is capable for online quality control. Spectroscopic NMR provides peaks (at given frequencies) corresponding to certain molecules of the sample under test. In addition, magnetic resonance imaging (MRI), which is usually considered as an extension of NMR, can further permit visualization of spatial distribution information on nuclear spins compared with NMR. MRI is performed with an NMR instrument equipped with magnetic gradient coils that can spatially gather the data thus creating two-dimensional (2D) and three-dimensional (3D) images that display areas having different physico-chemical properties with different contrasts. In other words, MRI provides spatial distribution of the signal due to presence of gradient in three axes.

Hyperspectral imaging

HSI is a new but rapidly growing technique that integrates spectroscopic and imaging techniques together to provide both spectral and spatial information simultaneously. It was originally developed for remote sensing (Goetz et al., 1985), and has currently emerged as a powerful tool for nondestructive assessment of food quality and safety. HSI can be carried out in reflectance, transmission, scattering, and transflectance or fluorescence modes in the field of food analysis. Hyperspectral images are 3D in nature, with two spatial dimensions and one spectral dimension. Therefore, HSI makes it possible to obtain the spectral information at each pixel of the hyperspectral images, and also the image information at each covered wavelength. Compared to conventional spectroscopic techniques,

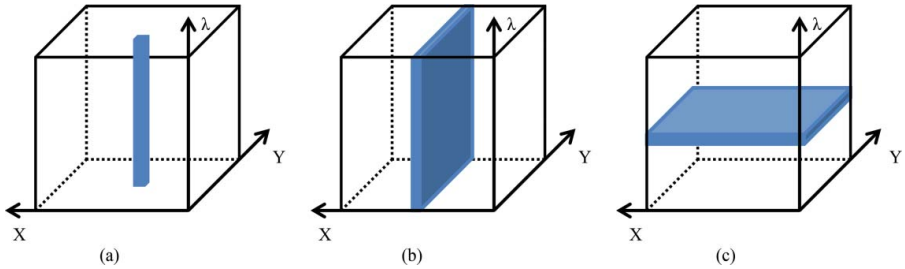

Figure 2. Different approaches to acquire hyperspectral cube: (a) point-scan, (b) line-scan, and (c) area-scan.

the added spatial dimension enables the mapping of chemical components in a sample (chemical imaging), which is particularly useful for nonhomogeneous samples.

Generally, there are three approaches for acquiring 3D hyperspectral cubes [hypercubes (x, y, λ)] (Fig. 2), namely, point-scan, line-scan, and area-scan methods. In the point-scan method (i.e., the whiskbroom method), a single point is scanned along two spatial dimensions (X and Y) by moving either the sample or the detector. A spectrophotometer equipped with a point detector is used to acquire a single spectrum for each pixel in the scene. Hyperspectral image data are accumulated pixel by pixel. The line-scan method (i.e., the push-broom method) is an extension of the point-scan method. Instead of scanning one point each time, this method simultaneously acquires a slit of spatial information as well as full spectral information for each spatial point in the linear field of view (FOV). A special 2-D image (y, λ), with one spatial dimension (Y) and one spectral dimension (λ), is taken at a time, and in this case, the hyperspectral systems need to use the imaging spectrographs that work in line-scan mode. A complete hypercube is obtained as the slit is scanned in the direction of motion (X). Different from the spatial-scan methods of point-scan and line-scan, the area-scan method (i.e., the band sequential method) is a spectral-scan method. This approach acquires a 2D single-band grayscale image (x, y) with full spatial information at once. A hypercube containing a stack of single-band images is built up as the scan is performed in the spectral domain. No relative movement between the sample and the detector is required for this method. Imaging systems using filters (e.g., filter wheels and electronically tunable filters) operate by the area-scan method. Since most food products are normally moved linearly along a production line, the line-scan method is well suited for online inspection of food quality and safety. Thus, the line-scan method is widely used for food analysis.

Applications in fat/FA analyses of muscle foods

Red meats

In the red meat industry, nonstandard quality of the raw material, mainly its fat content, plays a crucial role in the economic and legal aspects of the industry's production process. By having an insight into the basic chemical composition of a raw material, it is possible to plan a production process thoroughly and declare the nutritional value of the products on a label as is commonly desired by consumers for health-related issues. For instance, excessive fat production has been identified as one of the major concerns of the beef industry. Over the past two decades, beef consumption has declined steadily in developed countries, due in part to health-related concerns.

The FAs composition of meat contributes largely to the nutritional value of the product (Wood et al., 2008), and also influences the technological and sensory quality of meat (Wood et al., 2004). The main components of technological quality of red meats influenced by FAs are tissue firmness (hardness), shelf life, and flavor. The effect of FAs on firmness is due to the different melting points of the FAs in meat. In the C18 FA series, stearic acid (C18:0) melts at 69.6°C, oleic acid (C18:1) at 13.4°C, C18:2 at −5°C, and C18:3 at −11°C, which show that as the content of UFAs increases, the melting point declines. The effect of FAs on meat shelf life is explained by the propensity of UFAs to oxidize leading to the development of rancidity. There is also production of volatile, odorous, and lipid oxidation products contributing to meat flavor during cooking. The FAs composition of ruminants can vary greatly, depending on different factors such as animal breed (Bressan et al., 2011; Malau-Aduli et al., 1998, Perry et al., 1998), feeding regime (Aharoni et al., 1995; Noci et al., 2007), n-3 and n-6 addition (Herdmann et al., 2010), conjugated linoleic acids (CLAs) supplementation (Schiavon et al., 2010), age and body weight (Link et al., 1970; Maltin et al., 1998), and additive genetic factors (Oka et al., 2002; Pitchford et al., 2002; Nogi et al., 2011). Therefore, large-scale recording of fat content and FA information is critical for red meat industry. This section reviews the applications of NIRS, RS, NMR, and HSI techniques in prediction of fat content and FAs composition in red meats, namely, pork, beef, and lamb meat.

Fat content

Both marbling and intramuscular fat (IMF) are important parameters for description and evaluation of fat content in red meats. Marbling is defined as the amount and spatial distribution of visible white flecks of fat present within the lean in the carcass rib-eye region. It is generally accepted that an appropriate degree of marbling has a favorable effect on meat juiciness, tenderness, palatability, and flavor (Emerson et al., 2013; Platter et al., 2003; Thompson, 2004; Wheeler et al., 1994). Marbling is often considered as an important characteristic that directly affects consumers' consumption decisions. It is an important assessment index for categorizing the quality of carcasses and there is often a very high correlation between marbling score and meat price. The marbling degree of meat is largely variable, which can be dependent on many factors, such as animal breed, sex, diet, age, and weight at slaughter (Bosch et al., 2012; Correa et al., 2006; Olivares et al., 2009). However, marbling levels are

currently assessed by experienced assessors by visually comparing standardized charts with meat samples. This visual appraisal method is subjective and it is difficult to maintain consistency between different marbling assessors. IMF quantifies the fat found between muscle fiber bundles within the ribeye and is commonly determined by chemical extraction method. IMF content is also considered to be one of the most important traits determining the quality of meat (ElMasry et al., 2012), and it is a key factor that influences the sensory and cooking quality of meat and also the eating satisfaction of consumers (Fernandez et al. 1999b; Morlein et al. 2005). As marbling is an important parameter for red meats while with different features, its determination applications are summarized separately in this manuscript.

Evaluation of marbling scores of red meats. Marbling is a parameter based on the spatial distribution of visible white flecks of fat, so the point-detection spectroscopic techniques such as NIRS, RS, and NMR are commonly not suited. To our knowledge, only HSI technique has so far been applied to determine marbling scores of red meats. HSI system integrates both spectroscopic and imaging techniques together; therefore, it has advantages over conventional computer imaging technique for marbling analysis. Series of studies conducted at McGill University have shown great potential of HSI technique combined with advanced image processing methods for pork marbling analysis. Qiao et al. (2007) used the HSI technique (430–1000 nm) to determine marbling scores of pork for the first time. The authors first imaged the NPPC marbling standards (from 1.0 to 10.0) and extracted the image texture indices using the angular second moment (ASM), which were used as indicators of the uniformity degree and size of textures. Images of samples at 661 nm where the contrast between lean meat and marbling was more obvious were selected to estimate the marbling scores. The authors showed that ASM could successfully discriminate the marbling scores of pork except for the standard score 10.0. However, the predicted results were higher than those obtained subjectively with an error around 1.0, which was probably due to the stronger halation of the fresh pork samples compared to the digitalized marbling standards. Liu et al. (2012) improved the Qiao et al. (2007) study by considering marblings as kind of line patterns, which were extracted using the wide line detector (WLD) technique. The proportion of marbling (PM) obtained using the WLD analysis on digital color images of marbling standards was applied to determine marbling scores. The techniques allowed improved detection of marbling not only for the red samples (RFN and RSE quality grades, with typically good contrast) but also for the more difficult pales samples (PSE and PFN quality groups) which traditionally have presented difficulty in assessing marbling due to poor contrast and light reflective problems. Thus, the work showed the high potential of using the WLD technique for developing an automatic marbling score assessment system. In the same work, Liu et al. (2012) considered the use of PM calculated at three wavelengths, namely, red (720 nm), green (580 nm), and blue (460 nm) channels (RGB channels) to predict marbling scores. It was shown that although the PM at the three combined channels strongly correlated with marbling scores of pork samples, the value calculated at the blue channel alone was sufficient to predict marbling scores. The results imply that a simple spectral system could be designed and used for marbling scores assessment based on the WLD technique. Later, Huang et al. (2013) continued the work and compared assessment of pork marbling using the WLD and an image texture extraction technique based on an improved GLCM algorithm. PM was calculated as in previous studies whereas image texture feature index was obtained from the improved GLCM-based image textures. Unlike the earlier work, pork sample image features were extracted from the red, green, and blue channels as well the combined RGB channels. The predictive ability of WLD technique was compared with image texture analysis based on an improved GLCM technique. The authors demonstrated that the WLD-based technique performed better than the GLCM-based technique for marbling score determination. The work also confirmed that the combined RGB channel was suitable for predicting pork marbling scores. However, contrary to the Liu et al. (2012) study, the green channel was found to also have stronger predictive ability for pork marbling score. This could be attributed to the different marbling standards used in the studies. The green channel worked better when pork samples were used whereas the blue channel was better when the digitized NPPC standard was used.

More recently, in another study using HSI images between 900 and 1700 nm, Huang et al. (2014a) compared three image analysis techniques of Gabor filter, WLD, and spectral averaging for pork marbling analysis, which were used to extract the image indices of texture, line, and spectral features, respectively. The authors first applied the stepwise regression procedure to determine the optimal wavelengths, and then the multiple linear regression (MLR) models were built based on them. Their results revealed that Gabor filter gave the best prediction result, with the correlation coefficient in validation set (R_V) of 0.90, using the derivatives of image textures at 961, 1186, and 1220 nm, which indicated the feasibility of multispectral imaging (MSI) for online inspection of pork marbling.

Prediction of fat content of red meats. *Prediction of fat content using NIRS.* The ability of NIRS to predict fat content in meat was examined extensively by many researchers. The main studies reported on prediction of fat content in red meats during the last two decades are summarized in Table 1, with the prediction accuracy expressed in the terms of correlation coefficient (R), determination coefficient (R^2), standard error (SE), or root mean standard error (RMSE) in validation set, calibration set, and/or cross-validation of the calibration set. Different authors have reported different model accuracies for different meat species, either in laboratory tests or online determinations. The prediction accuracies can depend on the NIR spectroscopic instrumentation, measurement mode, spectral range, data analysis method employed, number of samples, and the nature of sample presentation (intact or minced) applied. Hardware of different NIRS instruments can be different leading to different detection accuracies. The initial studies worked with numerous filters to obtain the light of different wavelengths, whereas modern NIRS has monochromators that act as wavelength selectors, allowing samples to be scanned over an entire spectral region at a time. For instance, in the work

Table 1. Recent publications on prediction of fat content in red meats by using NIRS technique.

Meat species	Sample presentation	Measurement mode	Spectral range (nm)	Data analysis	CV (%)	Accuracy	References
Pork meat	Ground	Reflectance	1441, 1510, 1655, 1728, 1810	MLR	22.4	R_P: 0.94–0.98 SEP: 0.82–1.35%	Tøgersen et al. (1999)
	Intact	Reflectance	802–2500	PLSR	52.78	$R_C = 0.70$	Brøndum et al. (2000)
	Intact	Reflectance	400–1700	PLSR	70	SEC = 1.32% $R_P^2 = 0.61$, SEP = 0.6%	Chan et al. (2002)
	Emulsified	Reflectance Transmittance	1100–2500	MLR	36.71 36.71	SEP = 0.16–0.28% SEP = 1.12%	Lanza (1983)
	Intact	Reflectance	380–1700	MLR	—	$R_C^2 = 0.35$, SEC = 3.6 g/kg	Hoving-Bolink et al. (2005)
	Intact	Reflectance	400–2500	PLSR	—	$R_C^2 = 0.30$, SECV = 4.0 g/kg	
	Homogenized					$R_C^2 = 0.87$, SECV = 1.8 g/kg	Barlocco et al. (2006)
	Intact	Reflectance	800–2500	MPLS	33.33–54.54	R_P: 0.63–0.76 SEP: 0.37–0.40%	Savenije et al. (2006)
	Intact	Reflectance	700–1100	PLSR	53.41	$R_C = 0.98$, RMSEP = 0.59%	Hu et al. (2008)
	Homogenized	Reflectance	1100–2500	MPLSR	48.85	R_{CV}^2: 0.98–0.99 SECV: 0.35–0.36%	Zamora-Rojas et al. (2011)
	Intact	Reflectance	1600–2400	PLSR	28.4	R_V^2: 0.43–0.53 SECV: 1.77–1.79%	Roza-Delgado et al. (2014)
	Intact	Reflectance	400–1495	PLSR	51.34	$R_P^2 = 0.33$, SEP = 1.03 g/kg	Balage et al. (2015)
	Emulsified/Homogenized	Reflectance	1100–2500	MLR	36.71	SEP: 0.27–0.31%	Lanza (1983)
	Ground and freeze-dried	Reflectance	1100–2498	MPLSR	30.93	SECV = 7.82 g/kg	Sanderson et al. (1997)
Beef	Ground	Reflectance	1441, 1510, 1655, 1728, 1810	MLR	22.4	R_P: 0.96 SEP: 1.16–1.30%	Tøgersen et al. (1999)
	Intact	Reflectance	1100–2500	PLSR	—	R_{CV}^2: 0.78–0.85 RMSECV: 1.2–1.4%	Rødbotten et al. (2000)
	Minced	Reflectance	400–2500	MPLSR	—	$R_{CV}^2 = 0.96$ SECV = 44.8 g/kg	Cozzolino and Murray (2002)
	Intact	Reflectance	400–2500	MPLSR	96.88	$R_{CV}^2 = 0.89$ SECV = 46.9 g/kg	Cozzolino et al. (2002)
	Minced	Reflectance	400–2500	MPLSR	96.88	$R_C^2 = 0.92$ SECV = 43.4g/kg	Cozzolino et al. (2002)
	Ground and semi-frozen	Reflectance	1100–2500	PLSR	—	RMSECV: 0.48–1.11%	Tøgersen et al. (2003)
	Minced	Reflectance	400–2500	MPLSR	51.66	$R_{CV}^2 = 0.82$, SECV = 0.44%	Alomar et al. (2003)
	Ground and frozen	Reflectance	400–1700	PLSR	16.94 31.76	$R_V^2 = 0.83$–0.93 SEP: 2.15–2.28%	Anderson and Walker (2003)
	Homogenized	Reflectance	1100–2500	PLSR	24.15	$R_C^2 = 0.92$, SECV = 16.22g/kg	Prieto et al. (2006)
	Homogenized	Reflectance	1108–2493	MPLSR	45.79	$R_P^2 = 0.76$, SEP = 0.49%	Ripoll et al. (2008)
	Intact (*Limousin*)	Reflectance	1100–1800	PLSR	35	$R_C^2 = 0.43$	Prieto et al. (2011)
	Intact (*Aberdeen Angus*)	Reflectance	1000–1800	PLSR	33	SECV = 1.029 g/100 g	
	Ground				161.35	$R_C^2 = 0.75$ SECV = 0.477 g/100 g $R_P^2 = 0.998$ SEP = 0.986%; RPD = 17.37	Su et al. (2014)
	Minced	Reflectance	1100–2498	PLSR	31.31	$R_{CV}^2 = 0.819$, RMSECV = 0.557%	Cecchinato et al. (2012)
Lamb meat	Minced	Reflectance	400–2500	MPLSR	—	$R_{CV}^2 = 0.71$, SECV = 4.7 g/kg	Cozzolino and Murray (2002)
	Intact				—	$R_{CV}^2 = 0.18$, SECV = 8.1 g/kg	
	Intact	Reflectance	400–2498	PLSR	45	$R_{CV}^2 = 0.698$, SECV = 0.526%	Andres et al. (2007)
	Minced and freeze-dried	Reflectance	1100–2500	PLSR	57.4	SEP = 0.43%	Viljoen et al. (2007)
	Intact	Reflectance	350–2500	GA-PLSR	33.14	$R_P^2 = 0.69$, RMSEP = 1.60%	Pullanagari et al. (2015)

PLSR, partial least squares regression; MPLSR, modified PLSR; MLR, multiple linear regression; GA-PLSR, genetic algorithm–based partial least squares regression; R_P, correlation coefficient of prediction set; R_C, correlation coefficient of calibration set; R_P^2, determination coefficient of prediction set; R^2_{CV}, determination coefficient of cross validation; R^2_C, determination coefficient of calibration set; SEP, standard error of prediction set; SEC, standard error of calibration set; SECV, standard error of cross validation; RMSEP, root mean square error of prediction; RMSECV, root mean square error of cross validation; RPD, residual prediction deviation; CV, coefficient of variation.

conducted by Tøgersen et al. (1999), a filter wheel rotating at 20 Hz containing five interference filters was used for acquisition of reflectance spectra. Sample presentation also has an important effect on prediction accuracy. Cozzolino and Murray (2002) compared its effect on predictions of fat content in beef and lamb meat, and their results show that the minced presentation is a better way to analyze meat samples using NIRS, compared to intact presentation. Thus, the efficiency of NIRS in predicting fat content in meat is usually better with minced, ground, and homogenized samples than it is with intact samples. Further, the effect on prediction accuracy has also been studied for different grinding sizes, which concluded that the finer the grinding, the higher the prediction accuracy (Tøgersen et al., 2003). The number of samples used to develop calibration models also influences the prediction accuracy. The literature shows that the number of samples used by different authors varies mostly between 30 and 150. However, Zamora-Rojas et al. (2011) conducted a work on predicting the fat content of different Iberian pork muscles using a large data set ($n = 310/342$) with a wide range of reference values. The authors reported remarkable prediction with R_{CV}^2 and SECV in the range of 0.98–0.99% and 0.35–0.36%, respectively, for homogenized meat. Compared to other studies published in this field, the work ensured realistic robustness of the calibration models by using a large data set. Further, calibration models can be established based on different muscle types, which may consist of a single muscle from different carcasses, different muscles from a single meat species and even a mixture of ground meat of different species (Tøgersen et al., 1999). Depending on such difference, the prediction accuracy can also be different. Almost all the studies were conducted using the NIR reflectance spectra, except an early study reported by Lanza (1983), in which transmittance spectra were compared with reflectance spectra for fat content prediction in emulsified pork paste. Their results showed that the reflectance spectra between 1100 and 2500 nm gave more accurate prediction results than transmittance.

Several studies (Cozzolino and Murray, 2002; Hoving-Bolink et al., 2005; Barlocco et al., 2006; Roza-Delgado et al., 2014; Balage et al., 2015) showed poor modeling results for fat content prediction in intact meat samples. The reason can be attributed to the fact that NIR spectroscopic method is a point detection technique, which can only cover small information of the tested sample, and thus have limitation for nonhomogeneous sample, such as intact meat. Additionally, in intact meat samples, the muscle fibers or myofibrils themselves may act as optical fibers tending to conduct NIR light along their length by a series of internal reflections, absorbing more energy and giving less reflectance when comparing with homogenized meat, which may lead to poorer modeling results for intact meat samples. In a study conducted by Hoving-Bolink et al. (2005), two reasons for low prediction results were recognized: one is as mentioned earlier; the other reason is due to the limited variation of the tested samples in fat content. However, the authors stated in this work that by using a NIRS with a larger sampling area (laboratory system with a sampling area of ± 5 cm^2), a R_C^2 of 0.70 can be achieved.

Most of the reported studies dealing with the ability of NIRS to determine fat content of meat aimed at exploring the possibility to replace conventional laborious and time-consuming analysis, and were thus made under the laboratory conditions. Only three studies (Tøgersen et al., 1999; Tøgersen et al., 2003; Anderson and Walker, 2003) explored the prediction ability of NIRS for on-line determination of fat content in meat under industrial conditions. In Anderson and Walker's work (2003), they developed an on-line spectral analysis system for prediction of fat content in heterogeneous ground beef streams. The Perten diode-array type Vis/NIR spectrometer, which moved at 1.0 m/min was used to take reflectance measurements from the meat stream. The SEPs reported by the authors for the 27-kg block-sized samples and the entire 400-kg block were 2.15–2.28% and 0.70–1.05%, respectively. Similarly, good modeling results were also obtained in the two studies reported by Tøgersen et al. (1999, 2003) for ground meat. However, as to our knowledge, no work has been published on on-line prediction of fat content in intact meat under industrial conditions using NIRS technique.

Prediction of fat content using RS. Compared to the wide applications of NIRS in red meats, only limited studies have been reported on analyzing meat fats by RS technique. Using RS technique between 270 and 1900 cm^{-1} with line-focused 785 nm excitation, Beattie et al. (2007) conducted a study to classify the intact adipose tissues from four different species (pork, beef, lamb, and chicken). Four classical multivariate methods which consisted of partial least squares discriminant analysis (PLSDA), principal component linear discrimination analysis (PCLDA), Kohonen and feed-forward artificial neural networks were applied, and the best classification accuracy of 99.6% was obtained by performing PLSDA method in their work. Further, another study was reported on using the polymorphic features of fats detected by RS to discriminate their animal-fat origins (Motoyama et al., 2010). The authors found that a single Raman band at 1417 cm^{-1}, which is the characteristic band of β'-polymorph of fats, could successfully differentiate pork fats from beef fats. Moreover, based on the Raman spectra of the extracted fat, successful classification of seven different meat species (pig, cattle, sheep, fish, poultry, goat, and buffalo) and their salami products was obtained by Boyaci et al. (2014). As to our knowledge, no study has been reported so far on quantitative determination of fat content in red meats using RS.

Prediction of fat content using NMR. Many studies have shown the potential of using NMR and MRI to predict fat content in red meats. Sørland et al. (2004) investigated the feasibility of LF-NMR for determination of fat content within a series of minced beef and pork samples in both fresh and dry presentations. In this work, the multipulsed magnetic field gradient spin echo (m-PFGSE) was applied for NMR tests, and the authors observed that for fresh samples, the recording of the fat signal started when the water signal was suppressed to an insignificant amount using the m-PFGSE sequence, and when the protein signal decayed due to a short T_2 relaxation time. Based on that, good agreement was obtained between the NMR and reference chemical method, with R_C of 0.975 for fresh beef, and also high correlation shown between the NMR values predicted within fresh and dry pork. Brøndum et al. (2000) compared the performance of four spectroscopic instruments, which consisted of a fiber optic probe, a Vis/NIR reflectance spectrophotometer, a reflectance spectrofluorometer and a ^{1}H LF-NMR

for rapid determination of fat content of two intact pork muscles (*longissimus dorsi* and *semitendinosous*). Their results showed that LF-NMR with the inversion recovery sequence gave the best modeling result, with R_C and SEC of 0.77% and 1.13%, respectively, though still not accurate enough. Using microwave as the drying method, Keeton et al. (2003) investigated the potential of the SMART Trac NMR system for fat content prediction in a range of dried meats and meat products, which consisted of low-fat pork, high-fat ground beef, deboned chicken with skin, all-beef hot dogs and U.S. National Institute of Standards and Technology (NIST) standard reference material. Their work showed that the NMR system could provide results comparable with those obtained by the AOAC methods except for the results of the high-fat (30–50%) beef sample and the NIST standard. In addition, the authors also examined the effects of sample weight, drying temperature and sample temperature on NMR prediction, and indicate that some factors have adverse effects on fat prediction. Further, Leffler et al. (2008) reported a collaborative work on prediction of fat content in a variety of dried meats (beef, pork, chicken, and turkey) and processed meats (beef hot dog, pork sausage, and ham) by NMR operating at 0.47 Tesla. Statistical analysis for total fat yielded similar relative standard deviation for repeatability (RSD_r) and relative standard deviation for reproducibility (RSD_R) range of 0.74–4.08%, which demonstrates that NMR combined with microwave drying is an effective method providing results equivalent to AOAC Methods 960.39 (Soxhlet Ether Extraction) in raw and processed meat products. More recently, to quantify the fat content in the trapezius muscle of live cattle, Nakashima (2015) developed a prototype NMR scanner (4.1 MHz for protons), which includes an original single-sided permanent magnet with depth of investigation of 30 mm and a sensed region as compact as $19\times19\times16$ mm^3. A measurement error of as small as approximately 10 wt.% was achieved in this work, which indicated that the prototype developed based on NMR would enable the *in vivo* fat content assessment of live cattle.

Compared to NMR spectroscopic method, MRI could provide additional spatial distribution information of fat in meat, which is an important trait in meat quality grading. An early study was reported for mapping the fat distribution in retail quality lamb using MRI technique with chemical shift selective imaging and T_1 weighting methods (Tingle et al., 1995). Their results show that T_1 weighting method has significant speed advantages over the chemical shift selective method for visualization of fat distribution in lamb, while for samples with very low fat content, the complete selectivity of the chemical shift technique would be required. Ballerini et al. (2002) reported a preliminary study for determination of fat content in heifer *longissimus dorsi* muscle by NMR image analysis. In this work, fat visualization was realized through a proposed segmentation algorithm, which included the steps of background suppression, nonuniformity removal by use of median filtering and fat extraction. Although the correlation between the mean fat content measured by chemical analysis and the presented method ($R_C = 0.77$) was higher than that achieved using the digital images of the same meat samples ($R_C = 0.58$), it is still considered low and the improving is needed. Recently, Lee et al. (2015) reported a study with beef by applying MRI technique to visualize and predict its IMF distribution. This study was based on the intensity difference between fat and lean meat content in the proton spin-lattice relaxation (T_1) weighted MRI image, which is considered to produce distinct results upon image processing. Their results showed a strong correlation between the MRI predicted and chemically measured IMF values, with R_C^2 of 0.98. The distribution uniformity of IMF within beef was evaluated by calculating their distribution and pixel size in the MRI images according to four levels of beef quality grade (1+, 1, 2, and 3), which is considered reliable for beef grading, however, the authors did not give the prediction accuracies for grading different levels of beef samples in their work.

In addition, MRI also shows great potential for fat analysis in pig carcass. Monziols et al. (2005) reported a method to quantify the amount of fat tissue in gradient echo magnetic resonance images, which provides segmentation of pure tissue and partial volume voxels, allowing separation of muscle and fat tissue including the fine insertions of intermuscular fat. Subsequently, Monziols et al. (2006) conducted another study to explore the suitability of LF-MRI for prediction of subcutaneous fat and intermuscular fat contents in pig carcasses and cuts. They obtained good agreements between the MRI measured and the reference values for total fat and subcutaneous fat, with R_C^2 in the range of 0.951–0.986 and 0.918–0.994, respectively. However, the R_C^2 for intermuscular fat content was low with the exception of belly ($R_C^2 = 0.798$–0.837).

Prediction of fat content using HSI. A number of studies have revealed HSI as a promising tool for prediction and visualization of IMF content in red meats. The first study was reported by Kobayashi et al. (2010) on applying HSI technique to predict and visualize fat content in beef. By extracting the mean spectra between 1000 and 2300 nm from the obtained hyperspectral images, PLSR model was established for fat prediction which gave a R_P^2, SEP, and (residual prediction deviation) RPD of 0.90, 4.81% and 2.84%, respectively. By applying the obtained model to each pixel of the hyperspectral images, the visualization map for showing the distribution of fat content in each sample was produced. Subsequently, another work was conducted to predict fat content in intact lamb meat originated from different breeds and different muscles (Kamruzzaman et al., 2012). Likewise, they extracted the mean spectra for model development, and based on the spectral information between 900 and 1700 nm, satisfactory prediction result was obtained, with R_P^2 and SEP of 0.88 and 0.40%, respectively. In addition, using the regression coefficients resulted from PLSR analyses, the feature wavelengths of 960, 1057, 1131, 1211, 1308, and 1394 nm were identified for quantifying fat content in lamb meat, and based on these determined optimal wavelengths, a simplified prediction model was obtained, with R_P^2 and SEP achieving 0.87% and 0.35%, respectively. The chemical images were also created in their work. Using the same HSI system with Kamruzzaman et al. (2012), Barbin et al. (2013) also obtained satisfactory results for prediction of fat content in both minced and intact pork, with R_P^2 and SEP of 0.95 and 0.37%, 0.83 and 0.76%, respectively. The wavelengths of 927, 937, 990, 1047, 1134, 1211, 1275, 1382, and 1645 nm were identified as feature-related for prediction of fat content in pork. Fig. 3(a) shows their distribution maps of fat content of

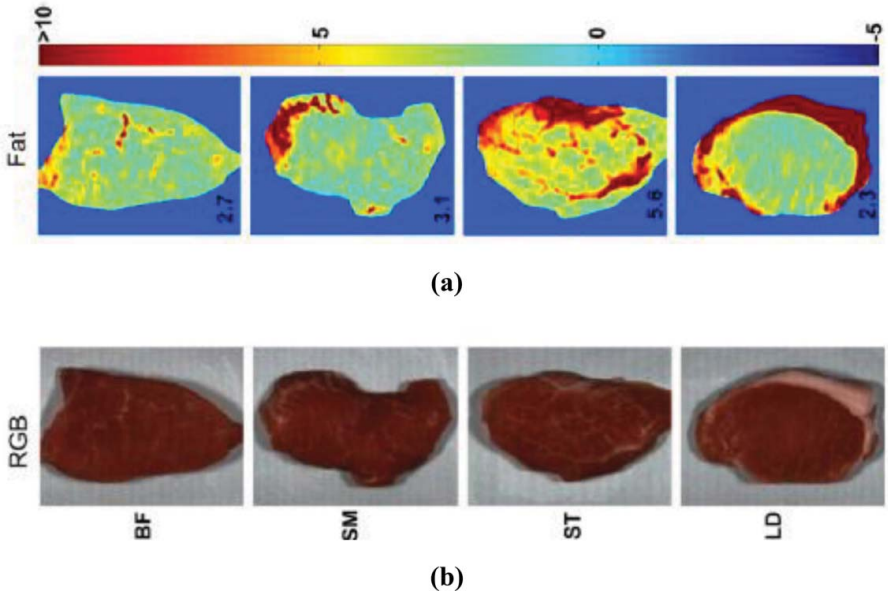

Figure 3. Images for intact pork samples: (a) concentration map of fat content and (b) pseudo-color image (Barbin et al., 2013).

each intact pork muscle created using the feature wavelengths, in accordance with the pseudo-color image composed by concatenating three selected wavelengths (1081, 1275, and 1329 nm) to represent the R, G, and B color channels in Fig. 3 (b). #3Similarly, ElMasry et al. (2013) obtained a R_P^2 and SEP of 0.84% and 0.65% for determination of fat content in intact beef, which was comparable with the aforementioned lamb and pork meat.

Other than only using the spectral information extracted from hyperspectral images, Liu and Ngadi (2014) and Huang et al. (2014b) explored using different image features combined with spectral information to determine the IMF content in pork. In the study reported by Liu and Ngadi (2014), they first extracted the visual IMF flecks on both sides of pork samples by using the WLD algorithm as mentioned earlier, and then the proportions of IMF fleck areas at critical wavelengths were used to predict the IMF content. The adjusted R_P^2 and RMSEP of 0.93% and 0.17% were achieved, respectively in this work, which is superior to the prediction accuracy reported by Barbin et al. (2013) with pork. Huang et al. (2014b) applied three image analysis techniques of spectral averaging, Gabor filter and improved GLCM to extract the raw spectral, texture-based spectral and textural characteristics of pork images, respectively. Using the first derivative of Gabor filtered spectra at 1193 and 1217 nm, the best prediction result was achieved with R_P of 0.86. More recently, Lohumi et al. (2016) reported a work on beef by using HSI technique over the spectral range of 400–1000 nm. In this study, three chemometric techniques including analysis of variance (ANOVA), spectral similarity measures of spectral angle measure (SAM), and Euclidian distance measure (EDM) were applied and compared. Their results showed that the spectral similarity measure methods outperformed the ANOVA based ratio-image method for IMF content analysis, in terms of overall classification and quantification accuracies. Their work achieved the R_C^2 of 0.91, 0.95, and 0.96 by using ANOVA, SAM, and EDM methods, respectively; however, it needs to be noted that the number of samples involved was small ($n = 24$) and also the models developed were not validated using independent samples. Regarding beef, Wold et al. (2011) reported a further study on on-line predicting fat content in beef trimmings using a calibrated NIR imaging scanner, which covered 15 wavelengths between 760 and 1040 nm with a spectral resolution of 20 nm. In their work, the satisfactory R_{CV} and RMSECV of 0.98 and 3.0% were achieved, and also the image for visualization of fat distribution was produced. Simulations based on true measurements indicate that the RMSEP decreases with increasing batch size and, for the case of 100 kg batches, it reached about 0.6%. The test on six batches of intact trimmings varying from 145 to 210 kg also gave similar fat estimates as an established microwave system obtained on the ground batches. The study reveals that the simplified HSI (MSI) is applicable to online estimate fat content in trimmings and also to control the production of batches to different target fat levels. More recently, Måge et al. (2013) developed and tested a system which consisted of a NIR imaging scanner, a conveyor belt, a flow weigher and grader and a host computer containing synchronizing software and a sorting algorithm for on-line sorting of meat (pork and beef) trimmings into categories with different fat levels by simulations and pilot-plant trials. The simulation results showed generally low bias (< 2%) for either category, which therefore indicates the great potential of their developed system for online implementation.

FAs composition

Prediction of FAs composition using NIRS. NIRS has shown its potential for predicting FAs composition in melted fats, adipose, and meat tissues with different grades of accuracy. Among different breeds of pork, Iberian pork is widely accepted by consumers owing to its special characteristics. In order to explore a rapid way to determine the FAs composition of Iberian pork, series of studies have been carried out using NIRS. An early study was reported by González-Martín et al. (2002), in which they investigated the capability of NIRS

(1100–2498 nm) with the so-called "*Cam-lock cups*" cells in transflectance mode for determination of FAs composition in the subcutaneous fat of Iberian pigs. In this work, two methods for collecting the total reference fat were compared, namely, extraction with solvents and microwave melting. With the fat extraction by solvents, their results show that the NIRS technique allows the determination of 12 individual FAs of C12:0, C14:0, C16:0, C16:1, C17:0, C17:1, C18:0, C18:1, C18:2, C18:3, C20:0, and C20:1, and total SFAs, mono-unsaturated FAs (MUFAs) and poly-unsaturated FAs (PUFAs) with R_C^2 of 0.84, 0.70, 0.89, 0.75, 0.62, 0.66, 0.85, 0.91, 0.88, 0.77, 0.85, 0.66, 0.92, 0.89, and 0.90 respectively, and SECV for these FAs of 0.012%, 0.109%, 0.66%, 0.24%, 0.04%, 0.04%, 0.54%, 1.15%, 0.49%, 0.12%, 0.03%, 0.23%, 0.82%, 1.12%, and 0.52%, respectively. While using the fat extraction by microwave melting, the NIRS method only achieved satisfactory results with 6 individual FAs of C16:0, C16:1, C18:0, C18:1, C18:2, C18:3, and group FAs of total SFAs, MUFAs, and PUFAs with R_C^2 of 0.93, 0.70, 0.88, 0.90, 0.83, 0.63, 0.95, 0.92, and 0.82, and SECVs of 0.48%, 0.24%, 0.65%, 1.13%, 0.59%, 0.10%, 0.83%, 1.24%, and 0.69%, respectively. Subsequently, based on the same NIR instrument, González-Martín et al. (2003) compared the determination results of FAs in the intact subcutaneous fat and extracted subcutaneous fat of Iberian pigs, with the assistance of a standard reflectance fiber optic probe (1100–2000 nm) and "*Cam-lock cups*" (1100–2498 nm), respectively. The predictions using the fiber optic probe for intact samples gave the R_P^2 for C14:0, C16:0, C18:0, C18:1, C18:2, C18:3, and C20:1, total SFAs, MUFAs and PUFAs of 0.72, 0.94, 0.72, 0.79, 0.88, 0.55, 0.17, 0.90, 0.74, and 0.88, respectively, and SEP for these FAs of 0.11%, 0.60%, 0.84%, 1.20%, 0.77%, 0.11%, 0.30%, 1.18%, 1.21%, and 0.76%, respectively. The predictions for extracted samples by "*Cam-lock cups*" achieved the R_P^2 of 0.53, 0.93, 0.84, 0.85, 0.87, 0.49, 0.43, 0.97, 0.90, and 0.85 for the abovementioned FAs, with SEP of 0.13%, 0.59%, 0.58%, 0.97%, 0.77%, 0.12%, 0.24%, 0.66%, 0.75%, and 0.84%, respectively. Furthermore, González-Martín et al. (2005) applied NIRS with reflectance fiber optic probe to determine FAs composition in IMF of Iberian pork. Their results showed the multiple correlation coefficients (RSQs) of 0.785, 0.798, 0.788, 0.825, 0.762, 0.765, 0.696, 0.859, 0.878, 0.807, 0.943, 0.858 for individual FA of C14:0, C16:0, C16:1, C17:0, C17:1, C18:0, C18:1, C18:2, C18:3, and total PUFAs, MUFAs and SFAs, respectively, and SECV of 0.08%, 0.63%, 0.26%, 0.02%, 0.02%, 0.51%, 0.77%, 0.64%, 0.05%, 1.06%, 0.34%, and 0.70%, respectively. In addition, by rapid prediction of the four main FAs (C16:0, C18:0, C18:1, and C18:2) in Iberian pig adipose tissue samples, De Pedro et al. (2007) implemented NIRS (400–2500 nm) with a fiber optic probe as an integral part of Iberian pork quality control programs and/or traceability systems. In this work, they reported the SECV of 0.38%, 0.36%, 0.59%, and 0.23% for C16:0, C18:0, C18:1, and C18:2, respectively, which indicate the high potential of NIRS combined with the fiber optic probe for rapid FAs composition determination in Iberian pork analysis.

Apart from Iberian pork, there are also plenty of studies conducted on other breeds of pork using NIRS. Using Fourier transform-NIR (FT-NIR) reflectance and transmission between 11000 and 4000 cm^{-1} (900–2500 nm), Ripoche and Guillard (2001) conducted an exploratory study to determinate the FAs composition in pork fat slices and extracts. Their results showed the validity of NIR transmission to estimate total SFAs, MUFAs, and PUFAs, and individual FA of C16:0, C18:0, C18:1, and C18:2 in pork fat extracts with high R_{CV}^2 values, while the predictions using NIR reflectance for direct measurements on fat slices were less good, which only gave R_{CV}^2s between 0.69 and 0.79 for total SFAs and PUFAs, and individual FAs of C18:1 and C18:2 (Table 2). Based the NIR transflection spectra between 400 and 2500 nm, Gjerlaug-Enger et al. (2011) tested the FAs composition and IV of melted subcutaneous fat of pig carcasses. They reported superior prediction results for total SFAs, MUFAs, PUFAs, and IV, with R_P^2 and SEP of 0.95 and 0.49%, 0.97%, and 0.65%, 0.99% and 0.34%, and 0.97% and 1.22%, respectively. Good prediction results were also obtained for individual FA of C18:2 *n*-6, C16:1 *n*-7, C18:0, C18:1 *n*-9, and C16:0, with R_P^2 and SEP of 0.84% and 0.87%, 0.89%, and 0.10%, 0.96% and 0.64%, 0.94% and 0.44%, and 0.98% and 0.29%, respectively. By employing a relatively large data set of samples collected from 155 batches of pig carcasses, Müller and Scheeder (2008) reported the R_P^2 of 0.98, 0.88, and 0.96 concomitant with the relative SEP of 0.9%, 1.6%, and 4.7% for prediction of total SFAs, MUFAs, and PUFAs, respectively by applying NIRS in homogenized fat tissue.

For intact fat tissue, Prieto et al. (2014) tested the ability of NIR reflectance technique (400–2498 nm) to estimate the FAs composition and IV in intact subcutaneous fat of pigs fed reduced-oil corn dried distillers grains with solubles (cDDGS) at 4°C and 35°C. They obtained good results for prediction of the proportions of total SFAs, MUFAs, PUFAs, *n*-3, and *n*-6 FAs and individual FAs of C16:0, C18:1, C18:2 *n*-6, and C18:3 *n*-3 (R_C^2s: 0.80–0.89; RMSECVs: 0.21–1.37% total FA) at both cold (4°C) and warm (35°C) temperatures. The R_C^2 and RMSECV for IV were 0.90% and 1.66%, and 0.87% and 1.80%, respectively, with cold and warm samples, respectively. However, in this work, the acquisition of NIR spectra needs assistance of a special sampling device with samples cut to 7 mm to fit it, which makes it unpractical for industrial use. The industry is more interested in simplification of the sampling presentation with low-cost instrumentation. For such purposes, Pérez-Juan et al. (2010) prove that NIRS with the fiber optic probe is promising. The authors collected the reflectance spectra between 909 and 2500 nm by direct application of a fiber optic probe transversally and longitudinally in each subcutaneous fat sample. Their results show that total SFAs, MUFAs, and PUFAs as well as oleic and stearic FAs can be predicted accurately ($R_P^2 > 0.70$). Additionally, the authors found no obvious prediction differences between positioning the probe transversally and longitudinally during tests.

Further efforts were also made on developing and optimizing NIRS technique for FAs characterization in live pigs and carcasses in the slaughterhouse. Based on spatially resolved NIR transmission spectroscopy, Sørensen et al. (2012) reported a measurement method to determine porcine carcass fat quality as a function of the distance to the skin by estimating its IV, which is capable of performing on-line at full production speed (approximately 1000 carcasses per hour). The authors found that the IV of porcine carcass varied as a function of feeding regime and fat depth. By using interval PLS (iPLS) regression

Table 2. Recent publications on prediction of FAs composition in red meats by using NIRS technique.

Meat species	Sample presentation	Measurement mode	Spectral range (nm)	Data analysis	FAs	CV (%)	Accuracy	References
Pork	Fat extracts	Transmission	900–2500	PLSR	C16:0/C18:0	—	R_P^2=0.86/0.88 RMSEP=0.49/0.63%	Ripoche and Guillard (2001)
					C18:1	—	R_P^2=0.98 RMSEP=0.58%	
					C18:2	—	R_P^2=0.81 RMSEP=0.51%	
					Total SFAs/MUFAs/PUFAs	—	R_P^2=0.94/0.98/0.98	
					C18:1		RMSEP=0.66/0.60/0.50%	
	Fat slices	Reflectance	900–2500	PLSR		—	R_P^2=0.72 RMSEP=4.3%	
					C18:2	—	R_P^2=0.79 RMSEP=2.7%	
					Total SFAs/PUFAs	—	R_P^2=0.67/0.62	
					C16:0/C18:0		RMSEP=3.1/3.6%	
	Melted subcutaneous fat	Transflection	400–2500	MPLSR		6.03/14.36	R_P^2=0.98/0.96	Gjerlaug-Enger et al. (2011)
					C16:1 *n*-7		SEP=0.29/0.64%	
					C18:1 *n*-9	13.72/3.63	R_P^2=0.89/0.94	
					C18:2 *n*-6		SEP=0.10/0.44%	
						11.74	R_P^2=0.84	
					Total		SEP=0.87%	
					SFAs/MUFAs/PUFAs	7.67/3.90/11.51	R_P^2=0.95/0.97/0.99	
					IV		SEP=0.49/0.65/0.34%	
	Homogenized fat tissue					5.45	R_P^2=0.97	
	Intact				Total		SEP=1.22	
	subcutaneous fat at 35 °C	—	—	—	SFAs/MUFAs/PUFAs	—	R_P^2=0.98/0.88/0.96	Müller and Scheeder (2008)
					C16:0/C18:0		SEP=0.9/1.6/4.7%	Prieto et al. (2014)
		Reflectance	400–2498	PLSR		8.7/13.7	R_C^2=0.84/0.78	
					C16:1/C18:1/C20:1		RMSECV=0.88/0.80%	
						19.76/5.8/12.52	R_C^2=0.71/0.84/0.67	
					C18:2 *n*-6/C18:3 *n*-3		RMSECV=0.19/1.15/0.07%	
						10.3/32.92	R_C^2=0.83/0.81	
					n-3 FAs/ *n*-6 FAs		RMSECV=0.99/0.22%	
						31.75/10.2	R_C^2=0.80/0.83	
					Total		RMSECV=0.26/1.03%	
	Intact				SFAs/MUFAs/PUFAs	9.1/5.6/10.6	R_C^2=0.86/0.82/0.86	
	Subcutaneous				IV		RMSECV=1.37/1.23/1.08%	
	fat at 4 °C					5.9	R_C^2=0.87	
					C16:0/C18:0		RMSECV=1.80%	
		Reflectance	400–2498	PLSR		8.7/13.7	R_C^2=0.81/0.79	
					C16:1/C18:1/C20:1		RMSECV=0.92/0.74%	
						19.76/5.8/12.52	R_C^2=0.75/0.80/0.69	
					C18:2 *n*-6/C18:3 *n*-3		RMSECV=0.19/1.13/0.06%	
						10.3/32.92	R_C^2=0.84/0.81	
					n-3 FAs/ *n*-6 FAs		RMSECV=0.91/0.21%	
						31.75/10.2	R_C^2=0.82/0.86	
					Total		RMSECV=0.25/0.94%	
					SFAs/MUFAs/PUFAs	9.1/5.6/10.6	R_C^2=0.89/0.86/0.89	

(*Cntinued on next page*)

Table 2. (Continued).

Meat species	Sample presentation	Measurement mode	Spectral range (nm)	Data analysis	FAs	CV (%)	Accuracy	References
	Longitudinal subcutaneous fat cuts							
					IV		RMSECV=1.11/1.11/0.97%	
						5.9	R_C^2=0.90	Pérez-Juan et al. (2010)
					C14:0/C16:0/C18:0		RMSECV=1.66%	
		Reflectance	909–2500	PLSR		20/7/22	R_P^2=0.75/0.37/0.80	
					C18:1 *n*-9/C18:1 *n*-7		RMSEP=0.2/1.4/1.0%	
						15-Dec	R_P^2=0.93/0.41	
					18:2 *n*-6/18:3 *n*-6		RMSEP=1.1/0.3%	
	Transversal subcutaneous fat cuts					10-Aug	R_P^2=0.71/0.51	
					CLA9_11/ CLA10_12		RMSEP=1.2/0.1%	
						128/132	R_P^2=0.90/0.87	
					Total		RMSEP=0.2/0.1%	
					SFAs/MUFAs/PUFAs	11/12/2010	R_P^2=0.81/0.94/0.73	
					C14:0/C16:0/C18:0		RMSEP=1.7/1.2/1.6%	
		Reflectance	909–2500	PLSR		20/7/22	R_P^2=0.72/0.41/0.84	
					C18:1 *n*-9/C18:1 *n*-7		RMSEP=0.2/1.4/0.9%	
	Adipose fat tissue					15-Dec	R_P^2=0.92/0.62	
	In vivo				18:2 *n*-6/18:3 *n*-6		RMSEP=1.2/0.2%	
						10-Aug	R_P^2=0.80/0.54	
					CLA9_11/ CLA10_12		RMSEP=1.0/0.1%	
	Carcass					128/132	R_P^2=0.86/0.87	
					Total		RMSEP=0.3/0.2%	
					SFAs/MUFAs/PUFAs	11/12/2010	R_P^2=0.77/0.93/0.79	Sørensen et al. (2012)
	Subcutaneous fat cuts with skin				IV		RMSEP=1.9/1.2/1.4%	
	Skin-free subcutaneous fat cuts	Transmission	1100–2200	iPLSR		5.51	RMSECV=1.44 g	Pérez-Marín et al. (2009)
	Transverse section of subcutaneous fat	Reflectance	450–2300	MPLSR	C16:0/C18:0			
					C18:1	11.5/13.8	SECV=1.24/0.67%	
					C18:2	6.5	SECV=1.42%	
	Extracted subcutaneous fat with solvents				C16:0/C18:0	8.5	SECV=0.36%	
			450–2000		C18:1		SECV=0.82/0.94%	
					C18:2		SECV=1.48%	
					C16:0/C18:0		SECV=0.55%	
			450–2300		C18:1		SECV=0.89/0.57%	
					C18:2		SECV=1.44%	
					C16:0/C18:0		SECV=0.47%	
	Extracted subcutaneous fat by microwave melting		450–2300		C18:1		SECV=0.81/0.57%	
					C18:2		SECV=0.99%	
					C16:0/C18:0		SECV=0.58%	
			1100–2300		C18:1		SECV=0.65/0.54%	
	Intact subcutaneous fat				C18:2		SECV=1.05%	
							SECV=0.35%	González-Martín et al. (2002)

Iberian pork		Transflectance	1100–2498	MPLSR	C12:0/C14:0/C16:0 /C17:0/C18:0/C20:0	—	R_C^2=0.84/0.70/0.89 /0.62/0.85/0.85 SECV=0.012/0.109/0.66 /0.04/0.54/0.03%	
	Extracted subcutaneous fat				C16:1/C17:1/C18:1 /C20:1 C18:2/C18:3	—	R_C^2=0.75/0.66/0.91/0.66 SECV=0.24/0.04/1.15/0.23%	
					Total SFAs/MUFAs/PUFAs		R_C^2=0.88/0.77 SECV=0.49/0.12%	
					C16:0/C18:0	—	R_C^2=0.92/0.89/0.90 SECV=0.82/1.12/0.52%	
	IMF	Transflectance	1100–2498	MPLSR	C16:1/C18:1	—	R_C^2=0.93/0.88 SECV=0.48/0.65%	
					C18:2/C18:3	—	R_C^2=0.70/0.90 SECV=0.24/1.13%	
					Total SFAs/MUFAs/PUFAs	—	R_C^2=0.83/0.63 SECV=0.59/0.10%	
					C14:0/C16:0/C18:0	—	R_C^2=0.95/0.92/0.82 SECV=0.83/1.24/0.69%	González-Martín et al. (2003)
		Reflectance	1100–2000	MPLSR	C18:1/C20:1	13.28/10.13 /18.34	R_P^2=0.72/0.94/0.72 SEP=0.11/0.60/0.84%	
	Adipose tissue				C18:2/C18:3	5.65/22.46	R_P^2=0.79/0.17 SEP=1.20/0.30%	
	Ground beef				Total SFAs/MUFAs/PUFAs	24.94/26.56	R_P^2=0.88/0.55 SEP=0.77/0.11%	
					C14:0/C16:0/C18:0	12.10/5.38 /24.30	R_P^2=0.90/0.74/0.88 SEP=1.18/1.21/0.76%	
					C18:1/C20:1	13.28/10.13 /18.34	R_P^2=0.53/0.93/0.84 SEP=0.13/0.59/0.58%	
		Reflectance	1100–2498	MPLSR	C18:2/C18:3	5.65/22.46	R_P^2=0.97/0.24 SEP=1.20/0.30%	
					Total SFAs/MUFAs/PUFAs			
	Ground beef				C14:0/C16:0/C17:0 /C18:0	24.94/26.56	R_P^2=0.87/0.49 SEP=0.77/0.12%	
						12.10/5.38	R_P^2=0.97/0.90/0.85	González-Martín et al. (2005)
					C16:1/C17:1/C18:1	/24.30	SEP=0.66/0.75/0.84%	
		Reflectance	1100–2000	MPLSR		13.85/6.68	RSQ=0.785/0.798/0.825	
					C18:2/C18:3	/31.25/10.28	/0.765; SECV=0.08/0.63 /0.02/0.51%	
					Total SFAs/MUFAs/PUFAs	16.35/23.81	RSQ=0.788/0.762/0.696	
					C16:0/C18:0	3.29	SECV=0.26/0.02/0.77%	
					C18:1	33.39/47.22	RSQ=0.859/0.878	
					C18:2		SECV=0.64/0.05%	
					C14:0/C16:0/C18:0		RSQ=0.858/0.943/0.807	
	Minced beef					7.19/3.08	SECV=0.70/0.34/1.06%	De Pedro et al. (2007)
					C18:1	/34.02		
		Reflectance	400–2500	—		—	SECV=0.38/0.36%	
					C18:2/C18:3	—	SECV=0.59%	Realini et al. (2004)
Beef						—	SECV=0.23%	
		Reflectance	400–2498	PLSR	Total SFAs/UFAs	16.34/4.68 /18.09	R_P^2=0.23/0.10/0.91 SEP=0.43/0.76/1.2%	
					C14:0/C16:0/C17:0 /C18:0	10.06	R_P^2=0.92 SEP=1.27%	

(*Cntinued on next page*)

Table 2. (Continued).

Meat species	Sample presentation	Measurement mode	Spectral range (nm)	Data analysis	FAs	CV (%)	Accuracy	References
						37.40/53.49	R_P^2=0.04/0.93	
					C16:1*cis*9/ C18:1*trans*		SEP=0.60/0.07%	Sierra et al. (2008)
					C18:1*cis*9/ C18:1*cis*11	6.62/8.76	R_P^2=0.87/0.90	
							SEP=1.16/1.18%	
		Transmittance	850–1050	MPLSR	C18:2*n*-6/ C20:4*n*-6	74.47/54.73	R_{CV}^2=0.80/0.83/0.78/0.74	
						/61.11/46.43	SECV=0.016/0.115/0.005	
	Ground beef				Total BFAs/CLAs		/0.055%	
						67.50/60.98	R_{CV}^2=0.79/0.31/0.87/0.77	
					Total SFAs/MUFAs/PUFAs	/65.23/43.75	SECV=0.013/0.043/0.089	
					C14:0/C16:0/C18:0		/0.010%	
						15.31/10.34	R_{CV}^2=0.147/0.005	
							SECV=0.027/0.003%	
					C16:1	52.02/65.06	R_{CV}^2=0.70/0.59	Cecchinato et al. (2012)
							SECV=2.91/1.61%	
					C18:1*n*-9 *cis*/*trans*	56.23/61.43	R_{CV}^2=0.84/0.85/0.24	
					/C18:1*n*-11 *trans*	/13.33	SECV=0.18/0.14/0.03%	
		Reflectance	1100–2498	PLSR	C10:0/C12:0/C17:0	49.9/33.0	R_{CV}^2=0.78/0.83/0.71	
						/29.4	RMSECV=0.014/0.135	
					C17:1		/0.138%	
						51.7	R_{CV}^2=0.82	
					C18:2 *cis*-9, *trans*-11		RMSECV=0.014%	
					/C20:2	41.7/37.1	R_{CV}^2=0.80/0.70	
					Total		RMSECV=0.22/0.02%	
					SFAs/MUFAs/PUFAs	3.2/29.7	R_{CV}^2=0.61/0.63/0.69	
					C16:0/C18:0	/36.6	RMSECV=0.54/0.50/6.02%	
	Intact beef					36.1	R_{CV}^2=0.73	
	(*Aberdeen Angus*)						RMSECV=3.81%	
					18:1Δ9 *cis*	39.1/42.4	R_{CV}^2=0.62/0.76	Mourot et al. (2014)
							RMSECV=3.14/0.86%	
					C18:2 *n*-6/C20:4 *n*-6	33.0/44.9	R_{CV}^2=0.80/0.80/0.61	
						/12.8	RMSECV=0.28/0.26/0.16%	
		Reflectance	400–2500	—		77.86/65.87	R_{CV}^2=0.94/0.89	
					C18:3 *n*-3/ C20:5 *n*-3		RMSECV=59.01/46.09 mg/100 g FM	
					/ C22:5 *n*-3		R_{CV}^2=0.92; RMSECV=86.61 mg/100 g FM	
						84.76	R_{CV}^2=0.44/0.01	
					PUFA *n*-6/*n*-3		RMSECV=15.68/3.84 mg/100 g FM	
	Intact beef					38.50/24.34	R_{CV}^2=0.49/0.06/0.17	
	(*Limousin*)						RMSECV=5.90/1.23/1.91	
					Total CLAs		mg/100 g FM	
						54.72/58.60	R_{CV}^2=0.58/0.37	
					Total	/33.73	RMSECV=22.09/8.32 mg/100 g FM	
					SFAs/MUFAs/PUFAs		R_{CV}^2=0.79; RMSECV=2.38 mg/100 g FM	
						36.78/47.65	R_{CV}^2=0.93/0.80/0.61	
					C14:0/C16:0/C18:0		RMSECV=108.76/116.03	
							/28.71 mg/100 g FM	
					C16:1/C18:1/C20:1	122.53	SECV=36/257/130 mg/100 g muscle	Prieto et al. (2011)
					C18:2 *n*-6/ C18:3 *n*-3	75.88/82.13	SECV=49/381/1.5	

Intact subcutaneous fat at 31 °C				/ C18:2 *cis*-9, *trans*-11	/37.32	mg/100 g muscle	
				/ C20:4 *n*-6/C20:5 *n*-3		SECV=13/4.4/4.9/4.0/2.4/0.4	
	Reflectance	1100–1800	PLSR	/ C22:6 *n*-3	42/34/32	mg/100 g muscle	
				Total *n*-6/*n*-3			
					39/34/50		
				Total SFAs/MUFAs/PUFAs		SECV=18/8.1	
				C14:0/C16:0/C18:0	20/25/41	mg/100 g muscle	
					/14/28/17	SECV=405/452/16	
				C16:1/C18:1/C20:1		mg/100 g muscle	
						SECV=26/146/62	
Intact				C18:2 *n*-6/ C18:3 *n*-3	18/19	mg/100 g muscle	
subcutaneous fat at 2 °C				/ C18:2 *cis*-9, *trans*-11		SECV=28/192/0.9	
				/ C20:4 *n*-6/C20:5 *n*-3	32/33/9	mg/100 g muscle	
				/ C22:6 *n*-3		SECV=13/3.3/2.9/4.0/2.7/0.9	
	Reflectance	1100–1800	PLSR	Total *n*-6/*n*-3	47/39/35	mg/100 g muscle	
				Total SFAs/MUFAs/PUFAs	43/40/47		
				n-3/C18:3 *n*-3		SECV=21/9.0	
				/C20:3 *n*-3	22/25/51	mg/100 g muscle	
Intact					14/29/26	SECV=235/240/17	
perirenal fat				CLNA/*c*9, *t*11, *t*15-C18:3/*c*9, *t*11, *c*15-C18:3		mg/100 g muscle	Prieto et al. (2012)
				CLA/*t*, *t*-CLA/*c*, *t*—		RMSECV=1.56/1.50/0.11	
				CLA/*c*9, *t*11-CLA	17/20	mg/g fat tissue	
						RPD=2.01/1.92/1.90	
				trans-MUFA	38/40/15	RMSECV=0.37/0.23/0.16	
				/*t*11-C18:1		mg/g fat tissue	
	Reflectance	400–2498	PLSR		51.6/53.4	RPD=2.03/1.96/2.00	
Intact subcutaneous fat				CLNA/*c*9, *t*11, *t*15—	/110.0	RMSECV=2.58/0.21/2.39	
Ground lamb				C18:3/*c*9, *t*11, *c*15-C18:3		/2.24 mg/g fat tissue	
				CLA/*t*, *t*-CLA/*c*, *t*-CLA/*c*9, *t*11-CLA	128.0/137.6	RPD=2.12/2.71/2.02/1.90	
					/122.8	RMSECV=8.83/4.24	
						mg/g fat tissue	
				trans-MUFA	56.6/70.08	RPD=2.52/2.02	
				/*t*11-C18:1	/55.3/59.9	RMSECV=0.37/0.24/0.16	
						mg/g fat tissue	
				n-6/C18:2 *n*-6	64.4/67.1	RPD=2.05/1.90/2.00	
						RMSECV=2.79/0.27/2.58	
				n-3/C18:3 *n*-3		/2.26 mg/g fat tissue	
	Reflectance	400–2498	PLSR		128.0/137.6	RPD=1.96/2.11/1.96/1.90	
				*c*9, *t*11, *t*15-C18:3	/122.8	/1.89	
				/*t*, *t*-CLA		RMSECV=9.13/4.42	
				trans-MUFA	56.6/70.08	mg/g fat tissue	Prieto et al. (2013)
				/ *t*11-C18:1	/55.3/59.9	RPD=2.43/1.95	
				cis-MUFA		RMSECV=0.20/0.16 %	
						RPD=1.95/2.00	
					64.4/67.1	RMSECV=0.08/0.07 %	
				C14:0/C16:0/C18:0		RPD=2.43/2.66	
						RMSECV=0.01/0.07 %	
Intact lamb	Reflectance	400–2498	PLSR	C16:1 Δ9 *cis*/ C17:1 Δ9 *cis*/ C18:1 Δ9 *cis*	28.79/29.39	RPD=2.12/2.09	
				/C18:1 Δ11 *cis*		RMSECV=1.29/0.87 %	
				C16:1 Δ9 *trans*/ C18:1 Δ9 *trans*/ C18:1 Δ10+Δ11 *trans*	40.20/42.98	RPD=1.97/1.97	

(*Cntinued on next page*)

Table 2. (Continued).

Meat species	Sample presentation	Measurement mode	Spectral range (nm)	Data analysis	FAs	CV (%)	Accuracy	References
					C18:2 *n*-6/C18:3 *n*-3 / C20:5 *n*-3 9*cis*, 11*trans*-CLA	68.00/53.58	RMSECV=2.12 % RPD=2.04	Guy et al. (2011)
						21.40/28.56	SECV=0.04/0.07/0.06 % RPD=2.29/5.28/3.82	
		Reflectance	400–2498	PLSR	Total LSFAs/BSFAs/*n*-6 /*n*-3/CLAs	9.48	SECV=0.01/0.003/0.11 /0.01 % RPD=3.12/3.33/6.12/2.50	
Lamb					Total *cis* MUFAs/*trans* MUFAs			
		Reflectance	400–2500	MPLSR	Total SFAs/MUPAs/PUFAs	64.79/49.62 /45.81	SECV=0.003/0.003/0.05 % RPD=3.67/2.33/2.33	
					Total SFAs/MUPAs/PUFAs	55.56/42.86 /45.93/41.86	SECV=0.03/0.01/0.002 % RPD=2.15/2.12/2.00	
						57.14/53.33 /73.71	SECV=0.01 % RPD=2.40	
						50.33/48.84 /44.44	SECV=0.13/0.01/0.04/0.01 /0.01 % RPD=6.46/3.33/2.43/2.08	
						62.16	/2.46 SECV=0.09/0.05 %	
						47.84/54.38 /43.75/39.13 /65.12	RPD=6.42/2.73 SECV=0.13/0.14/0.04 % RPD=6.78/6.81/3.00	Pullanagari et al. (2015)
						45.92/68.64	R_p^2=0.60/0.60/0.67 RMSEP=192.21/168.72 /27.86 mg/100 g meat	
						47.98/48.19 /36.02		
		Reflectance	350–2500	GA-PLS		31.98/32.93 /19.86		

Figure 4. Collection of NIR spectra in (a) live animals, (b) carcasses, and (c) fat samples over the skin (Pérez-Marín et al., 2009).

method, they obtained a low RMSECV of 1.44 g for predicting IV of the porcine adipose fat tissue online at a given measured depth, which indicates that their presented method can provide the abattoir new possibilities for meat/carcass grading and product development by using their fat quality information. Pérez-Marín et al. (2009) also conducted an exploratory work by using NIRS combined with a fiber-optic contact probe to predict four main FAs in Iberian pig fat, which included palmitic acid, stearic acid, oleic acid, and LA. In this work, five sampling modes were applied, namely from the live animal (Fig. 4(a)), from the carcass in the slaughterhouse (Fig. 4(b)), from a subcutaneous fat sample with skin (Fig. 4(c)), from a skin-free subcutaneous fat sample, and from a transverse section. They obtained the SECV of 1.24% *in vivo* analysis and 0.82% for carcass analysis for palmitic acid, 0.67% and 0.94% for stearic acid, 1.42% and 1.48% for oleic acid, and 0.36% and 0.55% for LA, respectively, which demonstrates the feasibility of NIRS for on-site inspection and control of Iberian pig FAs composition, both in the field and in the slaughterhouse.

Regarding beef, Realini et al. (2004) employed the NIRS technique (400–2498 nm) in reflectance mode to characterize the FAs composition of ground beef from grass-fed and grain-fed sources. Results from PLSR modeling showed accurate predictions for total SFAs and UFAs, with R_P^2 and SEP of 0.87% and 1.16%, and 0.90% and 1.18%, respectively. Good predictions were also observed for individual FAs of C18:0, C18:1, and C18:3, with R_P^2 and SEP of 0.91% and 1.2%, 0.92% and 1.27%, and 0.93% and 0.07%, respectively. However, the composition of other individual FA was poorly predicted in this work. Also with ground beef, Sierra et al. (2008) applied the NIR transmittance spectroscopy (850–1050 nm) to predict its FAs composition. Their results showed that the NIR transmittance spectra could predict some prominent FAs well, such as C14:0, C16:0, C16:1*cis*9, C17:0, C18:1*cis*9, and C18:1*cis*11, with R_{CV}^2s all over 0.76 (Table 2), and also some minor FAs of C15:0, C17:1*cis*9, and C18:1*cis*13 with R_{CV}^2 of 0.798, 0.817, and 0.797, respectively. For FA groups, the R_{CV}^2 obtained for total SFAs, total MUFAs and branched FAs were 0.837, 0.852, and 0.701, respectively. More recently, another study was reported by using reflectance NIRS between 1100 and 2498 nm to determinate FAs composition in minced beef samples (*longissimus thoracis* muscle), and good cross-validation results (Table 2) were obtained for total SFAs, MUFAs and PUFAs, 6 major FAs (C14:0, C:16:0, C16:1, C18:0, C18:1*n*-9 *cis*/*trans*, and C18:1*n*-11 *trans*), and also 6 minor FA (C10:0, C12:0, C17:0, C17:1, C18:2 *cis*-9, *trans*-11, and C20:2) (Cecchinato et al., 2012). However, Mourot et al. (2014) did not get satisfactory results in predicting FAs composition of ground beef by using the reflectance spectra over 400 and 2500 nm, and good cross validation results were achieved for individual FAs of C16:0, C18:0, and 18:1Δ9 *cis*, and FAs groups of total CLAs, SFAs, and MUFAs (Table 2), which the authors believe is due to the narrow range of reference data.

Apart from predicting FAs composition in ground beef, several studies have also been published on intact beef recently. Prieto et al. (2011) examined the capability of reflectance NIRS (1100–1800 nm) with assistance of a fiber optic probe to predict the FAs composition in intact beef on-line in the abattoir. Beef samples from two cattle breeds (crossbred *Aberdeen Angus* and *Limousin*) were used in their work, and statistically significant differences ($P < 0.001$) were observed in most FAs between these two breeds, with FA concentration being higher in *Aberdeen Angus* meat mainly. Their results showed moderate to high predictability for C16:0, C16:1, C18:0, C18:1 *trans*11, C18:1, C18:2 *n*-6, C20:1, C18:2 *cis*9,*trans*11, total SFAs, MUFAs, and PUFAs in *Limousin* samples, with R_C^2 and SECV (g/100 g muscle) of 0.69 and 0.146, 0.69 and 0.028, 0.71 and 0.062, 0.70 and 0.0081, 0.76 and 0.192, 0.65 and 0.013, 0.71 and 0.0009, 0.71 and 0.0029, 0.68 and 0.235, 0.75 and 0.240, 0.64 and 0.017, respectively. However, the results for predicting FAs in *Aberdeen Angus* samples were not as good as in *Limousin* samples. Using the Vis/NIR reflectance spectroscopy (400–2498 nm), studies were also reported on prediction of the contents of PUFAs and biohydrogenation products in the subcutaneous fat of beef cows fed different diets (Prieto et al., 2012; 2013). Prieto et al. (2012) first compared the modeling results of NIR reflectance scannings at warm and cold temperatures (31 and 2°C), and suggested 31°C as a proper temperature for NIRS tests with beef fat. The modeling results with RPD very close or over 2.0 were summarized in Table 2, and from it, we can observe that for *n*-3 PUFAs, only the sample temperature of 31°C gave accurate results. In addition, it is notable that in this work the authors also studied the possibility of NIR reflectance spectra in predicting the ratio of *n*-6/*n*-3 which is an important parameter in a healthy diet; however, the RMSECV and RPD only reached 0.98 mg/g fat tissue and 1.51, and 1.07 and 1.44 at 31 and 2°C, respectively. Subsequently, based the same NIRS instrument, Prieto et al. (2013) compared prediction of total PUFAs and their biohydrogenation products in perirenal fat and subcutaneous fat from cattle fed sunflower or flaxseed, and modeling results with RPD very close or over 2.0 are shown in Table 2. From Table 2, it can be concluded that NIR reflectance spectra are more reliable for predicting FAs composition of perirenal fat.

Information on the FA analysis of lamb meat by NIRS is relatively scant. As to our knowledge, only two studies were published on lamb meat since recently. Guy et al. (2011) compared the feasibility of Vis/NIR reflectance spectroscopy

(400–2500 nm) in predicting FAs composition of ground and intact lamb meat (*Longissimus lumborum*). Their results showed much more accurate quantitative models for ground lamb meat than for intact meat samples, which is in accordance with the aforementioned results summarized for fat content prediction using NIRS. In this work, the obtained SECVs and RPDs for groups of total SFAs, MUFAs, PUFAs, linear saturated FAs (LSFAs), branched saturated FAs (BSFAs), *cis* MUFAs, *trans* MUFAs, *n*-6 PUFAs, *n*-3 PUFAs and CLAs and individual FAs of C14:0, C16:0, C18:0, C16:1 Δ9*cis*, C17:1 Δ9*cis*, C18:1 Δ9*cis*, C18:1 Δ11*cis*, C16:1 Δ9*trans*, C18:1 Δ9 *trans*, C18:2 *n*-6, C18:3 *n*-3, C20:5 *n*-3, C18:1 Δ10 + Δ11 *trans*, 9*cis*,11 *trans*-CLA were good for ground lamb (shown in Table 2), which indicate the great potential of NIRS for analyzing the FAs composition of ground meat. However, the best R_{CV}^2 achieved for intact lamb meat was only 0.53 and also all RPDs obtained lower than 2.0. More recently, another study was reported by using a high intensity contact probe connected to a Vis/NIRS (350–2500 nm) to quantify the FAs composition of lamb meat under commercial abattoir conditions (Pullanagari et al., 2015). However, the modeling results obtained were inferior, as the highest R_P^2 only achieved 0.73 among all FA groups and individual FAs. As shown in Table 2, the prediction results for total SFAs, MUFAs and PUFAs by using the genetic algorithm (GA)–based partial least squares (GA-PLS) method were only achieved with R_P^2 of 0.60, 0.60, and 0.67, respectively.

In addition, other than working on individual species of red meat as above, Mourot et al. (2014) investigated the possibility of developing universal equations for homogenized ruminant meats to predict their FAs composition. The reflectance spectra over the spectral range of 400–2500 nm were collected for homogenized beef and lamb meat for model development, and based on that, the R_{CV}^2 and RPD values of 0.68 and 1.76, 0.90 and 3.11, and 0.80 and 2.24 were obtained for LA, total CLAs and PUFAs, respectively, which indicated the robustness of NIRS for FA prediction in red meats and also the commonalities among different species of red meats.

Prediction of FAs composition using RS. The first trial of using RS to predict the FAs composition of unextracted adipose tissue was reported by Beattie et al. (2006). The samples used in their investigation were subcutaneous adipose tissue dissected from above the *Longisimus dorsi* in the position of the 12th rib for beef, beef, and lamb, and from above the breast for chicken. Their results showed that the bulk unsaturation parameters could be predicted successfully ($R_P = 0.97$, RMSEP = 4.6% of 4σ), with *cis* unsaturation, which accounted for the majority of the unsaturation, giving similar correlations. The total PUFAs was also well predicted with R_P and RMSEP of 0.97 and 4.0% of 4σ, respectively. However, it was not possible to find a good prediction model for *trans* unsaturation, which was explained to be due to the low range of relative abundances of *trans* unsaturated bonds in the adipose tissue (0.031, compared with 0.24 bonds per FA for *cis* unsaturated bonds). For individual FAs, the average RMSEP of the 18 most abundant FA was 11.9% of 4σ while the prediction errors for the five most abundant FA were all better than the average value (in some cases as low as RMSEP = 4.7% of 4σ). Subsequently, Olsen et al. (2007) conducted a study to compare the capability of RS (excitation wavelength at 785 nm) for FAs composition and IV prediction in intact pork adipose tissue and melted fat. Based on PLSR modeling method, they obtained for melted pork fat the R_{CV} and RMSECV (percentage of total FAs) of 0.99% and 0.6%, 0.96% and 1.0%, and 0.98% and 1.0%, 0.98 and 1.4 g for total SFAs, MUFAs, PUFAs, and IV, respectively, and for intact pork adipose tissue of 0.96% and 1.1%, 0.91% and 1.5%, and 0.95% and 1.5%, 0.97 and 1.8 g, respectively, which indicated no obvious difference between melted fat and intact adipose tissue. Their results suggest RS with a ball probe has great potential for online measurement of FAs composition in intact pork adipose tissue. However, in another study on intact pork adipose tissue, relatively inferior results were obtained with R_C^2 and RMSECV (percentage of total FAs) of 0.50% and 2.24%, 0.57% and 2.28%, and 0.72% and 1.17%, 0.69 and 2.00 g for prediction of total SFAs, MUFAs, PUFAs and IV, respectively (Lyndgaard et al., 2011). Further, Olsen et al. (2008) applied RS to quantify *n*-6 and *n*-3 FAs in intact pork adipose tissue and melted fat. Based on PLSR method, they obtained the R_{CV} and RMSECV (percentage of total FAs) of 0.97% and 0.99%, 0.91% and 0.23% for *n*-6 and *n*-3 FAs, respectively in melted fat, and 0.95% and 1.43%, and 0.87% and 0.27%, respectively, in intact pork adipose tissue. More recently, Berhe et al. (2016) reported a study on predicting FA groups and individual FAs in intact pork backfat using RS (200–1800 cm^{-1}) equipped with a 785 nm laser. In this work, they separately recorded Raman spectra from the inner and outer layers of pork backfat, and found that the model validation results for total SFAs, MUFAs, PUFAs, and IV with the inner layer were slightly better than those with the outer layer of backfat. The average R_{CV}^2 achieved for total SFAs, MUFAs, PUFAs, and IV was 0.84, 0.81, 0.90, and 0.89, respectively, and also good agreements were obtained for individual FA of C16:0, C18:1 *cis* Δ9, C18:2 *cis* Δ9,12, and C18:3 *cis* Δ9,12,15 with R_{CV}^2 of 0.89, 0.82, 0.90, and 0.87, respectively. Moreover, Olsen et al. (2010) studied the stability of a calibration model established from a Raman instrument for IV prediction of pork adipose tissue during a period of 3 years. The authors found that although with the fiber optic cable changed, the output of the laser reduced to 60% and the samples collected from different parts of the carcass, a good agreement could be obtained three years later by aligning the peak positions and preprocessing Raman data together with a selection of wavelengths/wavenumbers gave, which shows that a quantitative use of Raman instruments are robust over time.

As to our knowledge, the only work on using RS technique to predict FAs composition in muscle meat was reported by Fowler et al. (2015), in which a handheld Raman device (300–2100 cm^{-1}) with a 671 nm laser was used to quantify the FAs composition in intact lamb M. *longissimus lumborum*. Their results indicate that there is a good agreement between the measured and Raman predicted total PUFAs ($R_C^2 = 0.93$), while not satisfactory for total MUFAs and SFAs ($R_C^2 < 0.60$). Compared to the modeling results obtained with the adipose tissue, the predictive ability of RS for FAs composition in muscle meat is inferior, which is probably due to that measuring adipose tissue avoids the need to discriminate between meat and fat spectra to remove contributions from overlapping protein vibrations on the fat signals which can arise when muscle meat is measured.

Prediction of FAs composition using NMR. The reports on using NMR-based technique for quantification of FAs composition in meats are rare. As to our knowledge, only two studies regarding CLAs prediction were published. Maria et al. (2010) utilized ^{1}H NMR technique to measure the relative quantities of CLAs of in the extracted fat of beef and subcutaneous samples, and obtained a good correlation ($R_C = 0.97$) between the CLAs measured by GC and NMR. However, it needs to be noted that only 12 samples were employed in this model, which implied that the model established might not be robust enough. More recently, another study was reported to quantify the absolute CLAs content (mg/100 g meat) in 41 beef ribeye steaks by using ^{1}H NMR along with a new simple and fast lipid extraction protocol (Prema et al., 2015). The obtained R_C of 0.96 suggests very good agreement between data obtained by this rapid extraction/NMR analysis method and the conventional chemical analysis method, which indicates the capacity of ^{1}H NMR for rapid determination of CLAs content in the extracted beef. However, till now, no studies have been published for FAs prediction in intact meats using NMR-based techniques.

Prediction of FAs composition using HSI. The studies on using HSI technique to predict FAs composition in red meats are scant. Only one study was found published, in which the potential of NIR HSI system (1000–2300 nm) was investigated for prediction and visualization of the FAs composition in beef (Kobayashi et al., 2010). In this work, the PLSR models were established using the mean spectra extracted from the hyperspectral images, and satisfactory results for were obtained for total SFAs and UFAs, with R_P^2, SEP, and RPD of 0.87%, 1.69%, and 2.43%, 0.89%, 3.41%, and 2.84%, respectively. For individual FA of myristic (C14:0), palmitic (C16:0), stearic (C18:0), myristoleic (C14:1), palmitoleic (C16:1), oleic (C18:1), and linoleic (C18:2), the R_P^2 and RPD varied in the range of 0.68–0.89 and 1.69–2.85, respectively. This study shows that HSI can be a promising tool for FAs composition analysis of red meats, and the results are encouraging for HSI to be applied to other species of red meats.

Chicken meat

Consumption of chicken has increased in many countries not only because it is a lean meat, perceived as being health-promoting due to its lower calorific value per kg, but also that it is considered to be a better source of PUFAs compared with meat from cattle and sheep, including the key *n*-3 FAs (Jahan et al., 2004). However, unlike the extensive work with red meats, only a small number of studies have been conducted with chicken meat on fat content and FAs composition analyses by using the four mentioned techniques. Until now, only studies using NIRS and NMR techniques have been reported for prediction of fat content in chicken meat and NIRS for FAs composition.

Fat content

Prediction of fat content using NIRS. Based on the NIR reflectance values at 1680, 1722, 1818, 2270, and 2336 nm, an early study was conducted by Valdes et al. (1989), and they reported a R_C^2 and SEC of 0.95 and 2.0 g/kg for ground and freeze-dried chicken carcass samples. Renden et al. (1986) exploited the capability of reflectance NIRS (1445–2310 nm) in predicting the fat content of homogenized whole-carcass of mature dwarf hens, and good agreement was obtained between the NIRS predicted fat and actual chemical values, with R_P^2 of 0.96. Using the reflectance spectra between 400 and 2500 nm, Cozzolino et al. (1996) obtained similar accuracy with R_C^2 and SEC of 0.95 and 4.5 g/kg for model calibration with minced chicken breast meat. Abeni and Bergoglio (2001) reported a higher accuracy with R_{CV}^2 and SECV of 0.97% and 0.24% for fat content determination in freeze-dried and minced chicken breast muscle, which was probably due to the removal of water effect by freeze-drying. By employing a big variation of chicken carcass samples from three different genotypes, which consisted of fast-growing broiler, slow-growing broiler and a layer-type chicken, McDevitt et al. (2005) also obtained an acceptable result for fat prediction within dry and ground samples, with R_{CV}^2 and SECV of 0.93 and 17.23 g/kg. Cozzolino and Murray (2002) compared the ability of reflectance NIRS technique in predicting the fat content of minced and intact chicken meat, and obtained the R_{CV}^2 and RMSECV of 0.95 and 5.4 g/kg, and 0.45 and 9.0 g/kg for minced and intact chicken meat, respectively. Their study result with chicken meat is in accordance with red meats that reflectance NIRS technique gives better prediction results for minced sample than intact one.

Moreover, other than using the NIRS in reflectance mode, Windham et al. (2003) applied the transmittance NIRS technique over the spectral range of 850–1050 nm to measure the fat content of boned raw poultry breast muscle, trimmings, and raw finished product (chicken nuggets). In this work, the authors used two methods to develop the fat calibration model, namely direct use of the database supplied by the instrument manufacturer and collecting the samples from a local processing plant to establish the model themselves. With the two methods, they obtained an error of 0.70% and 0.33% for fat content calibration, respectively, and the corresponding SEP was 0.84% and 0.38%. The self-developed model was more accurate for fat content prediction in their work. The low errors obtained in this work supports that transmittance NIRS technique is powerful in the poultry processing industry for fat analysis in quality monitoring and processed product formulation.

Prediction of fat content using NMR. Only two studies were found reported on analysis of chicken fat by using NMR-based method. Based on spin echo sequence, Kövér et al. (1998) applied MRI technique to scan commercial broiler chickens at the age of 6, 7, 8, 10, and 16 and 20 weeks for tracing their pectoral, abdominal, and total fat volume changes. Their study demonstrated that changes found in the pectoral muscles as well as in total and abdominal fat volume were in good agreement with dissection data obtained at the slaughterhouse and also laboratory data based on the measurement of total body chemical composition in both sexes. Recently, Mitchell et al. (2011) exploited quantitative magnetic resonance (QMR) for measuring total body fat of live chickens. High correlation ($R_C^2 = 0.94$) was obtained between the data predicted by QMR and chemical analysis, however, the accuracy was low, with QMR method underestimating the percentage of total body fat by 34%.

FAs composition

Prediction of FAs composition using NIRS. Three studies were found published on determination of FAs composition in chicken meat recently. Berzaghi et al. (2005) tested the capability of NIR reflectance spectra between 1100 and 2498 nm for FAs composition determination in freeze-dried and ground breast meat of laying hens fed four different diets, a control and three diets enriched with different sources of *n*-3 PUFAs. Accurate cross-validation results were achieved for total SFAs, MUFAs, and PUFAs, and individual FAs of C16:0, C18:0, C18:1, C18:2 *n*-6, C20:4 *n*-6, and *n*-6, with R_{CV}^2 and SECV varying in the ranges of 0.89%–0.97 and 0.052%–0.165%, respectively. Similarly with freeze-dried and ground broiler chicken breast meat, Zhou et al. (2012) applied Vis/NIR reflectance spectroscopy (400–2498 nm) to determine its FAs composition, based on both absolute and relative (%) FA contents. Their results showed that calibrations based on the absolute FA content resulted in better performance than those based on the relative content. Satisfactory performance was obtained for most individual FAs and FA groups (based on the absolute content) except C18:3 *n*-6, C20:0, C20:2 *n*-6, and C24:1 *n*-9, with R_P^2 values between 0.83 and 0.97. Furthermore, to determine the effectiveness of the reflectance NIRS with assistance of fiber optic probe for on-line determination of FAs composition of chicken meat at the slaughterhouse, De Marchi et al. (2012) conducted a study on intact breast muscles over the spectral range of 350–1830 nm; however, no satisfactory prediction models were obtained in their work, with R_{CV}^2 less than 0.60 for all studied FAs.

Fish and fish oil

Fish has always been considered to be one of the most significant sources of nutrients for mankind. Over the past several decades, many studies have demonstrated the association between fish consumption and the decreased risk of diseases, such as cardiovascular disease (Stone 1996), ischemic heart disease, and stroke (Zhang et al., 1999). Fish are rich sources of long-chain *n*-3 PUFAs, such as EPA and DHA, which are acknowledged as the key nutrients attributed to the potential protective effects of fish consumption. Moreover, to be able to tailor fish quality for different markets in the future, there is also a great need for rapid and non-destructive analysis methods, supporting the instant documentation of the fat content and FAs composition in fish.

Current dietary guidelines recommend a daily intake of 0.5–1.0 g of EPA and DHA for primary and secondary prevention of coronary heart disease, and higher pharmacological doses are recommended for treatment of hypertriglyceridemia (Duda et al., 2009). However, low dietary intakes of long-chain n-3 PUFAs in some countries have resulted in the need for both dietary supplements and foods fortified with these FAs (Murphy et al., 2007; Sanguansri and Augustin, 2007). Fish oil contains a large amount of long-chain *n*-3 PUFAs, and thus has become one of the popular dietary supplements for consumers. The market of fish oil has rapidly expanded in recent years, and currently there are many brands of fish oil supplements available for consumers, most of which claim the active ingredients EPA and DHA on their labels. Rapidly increasing public demand for these products requires strict process control and high standards in quality assurance, which in turn requires simple, rapid, and accurate analytical techniques for monitoring these FAs both during and after production. This section reviews the recent research progress in analyzing fat content and FAs composition of fish and fish oil by using NIRS, RS, NMR, and HSI techniques.

Fat content

Prediction of fat content using NIRS. Based on NIRS technique, a wide range of studies have been reported on prediction of fat content in different species of fishes, with most studies carried out on trout and salmon fishes in reflectance mode. The detection of fat in fish by NIRS started with ground and freeze-dried samples first. An early study was reported by Gjerde and Martens (1987) on prediction of fat content in ground and freeze-dried rainbow trout (*Salmo gairdneri*) by using a 19-filter NIR instrument which covered the spectral range of 1445–2384 nm, and a SEC of 4.5 g/kg was obtained. Similar to the ground and freeze-dried of rainbow trout, Valdes et al. (1989) obtained R_C^2 and SEC of 0.78 and 1.4 g/kg for fat prediction by using the NIR reflectance values at 1722, 1734, 1778, 1818, and 1940 nm. Recently, Folkestad et al. (2008) reported a work on predicting fat content of farmed Atlantic salmon in both fillet and gutted states by using Vis/NIR reflectance spectroscopy (449–744 and 760–1040 nm). The R_{CV} and SECV of 0.83% and 1.58% were obtained for fish fillet samples, and the data range of 0.86%–0.90% and 0.68%–1.25% for gutted fish, respectively.

As mentioned above, NIRS in conjunction with the fiber optic probe has great potential for on-line determination of the chemical composition of foods. To exploit its feasibility in online predicting the fat content of Atlantic salmon, Isaksson et al. (1995) conducted a study with both ground and intact-farmed Atlantic salmon fillets. The RMSECV of 6.6 and 10.8 g/kg was obtained for ground and intact salmon fillets, respectively, which illustrated the high efficiency of NIRS with fiber optic probe. Further, based on the same NIR instrument with Isaksson et al. (1995), while with different type of fiber optic probe, Wold and Isaksson (1997) continued to exploit its capacity for predicting the average fat content of the whole Atlantic salmon, and R_{CV} and RMSECV of 0.87% and 1.12% was achieved, respectively. Recently, another study was reported on prediction of fat content in farmed Atlantic salmon using a portable Vis/NIRS (350–2500 nm) equipped with a contact probe (spot size: 10 mm) (Brown et al., 2014). In this work, three sampling presentations of minced Norwegian quality cuts (NQCs), intact NQCs and gutted fish with skin were included, and the prediction results with R_P^2 and SEP of 0.94% and 0.5%, 0.82% and 1.0%, and 0.77% and 1.2% were achieved, respectively, for small fish (weight: average ± SD of 1.4 ± 0.4 kg), and 0.86% and 0.7%, 0.59% and 1.2%, and 0.49% and 1.5%, respectively, for large fish (weight: average ± SD of 4.2 ± 0.9 kg).

In addition to using the reflectance mode, several studies were also reported on applying NIR transmittance spectra to predict fat content in fish. Based on the NIR transmittance spectra between 850 and 1050 nm, Sollid and Solberg (1992) measured the homogenized Atlantic salmon paste of 23-mm

thickness, and achieved a SECV of 0.49%. Wold et al. (1996) exploited the ability of NIR transmittance spectroscopy in predicting the average fat content of farmed Atlantic salmon fillets with skin and scales. The authors collected the NIR transmittance spectra from the upper part of the fish, just behind the dorsal fin to represent the average fat content of whole salmon, and based on the transmittance values at 930, 870, 890, 910, 1010, 970, 990, 1050, and 950 nm, satisfactory prediction results were obtained, which demonstrate the usefulness of NIR transmittance spectra in prediction of fat content in fish.

Recently, some researchers also investigated the capacity of NIRS in predicting fat content of live fish. Solberg et al. (2003) conducted an exploratory research on the live, anaesthetized farmed Atlantic salmon first, using two different NIR instruments, namely, a grating monochromator instrument equipped with a fiber optic interactance probe (800–1098 nm), and a diode array instrument measuring diffuse reflectance (900–1700 nm). Their study showed that both methods resulted of the same accuracy, with R_{CV} and RMSECV of 0.90 and 14 g/kg. Folkestad et al. (2008) reported a better validation result for prediction of fat content in anaesthetized live-farmed Atlantic salmon, with R_{CV} and RMSECV of 0.94% and 1.0%, respectively. Both studies suggest the great potential of NIRS in estimating fat content of live fish, which would make it possible to monitor the feeding regime and determine the fat content of fish before slaughter for future product tailoring of different markets.

Except for trout and salmon, NIRS was also applied to quantify fat content in other fish species, such as halibut (Nortvedt et al., 1998), skipjack (Shimamoto et al., 2003), mackerel (Shimamoto et al., 2004) and tuna (Khodabux et al., 2007), and so on. The NIR transmittance spectra between 850 and 1048 nm were used to determine fat content in homogenized Atlantic halibut, and satisfactory cross validation result was obtained, with RMSECV of 2.7 g/kg (Nortvedt et al., 1998). Shimamoto et al. (2003) employed both portable and desktop NIR spectrophotometers (700–962 nm) to determine fat content in frozen skipjack, and concluded that the fat content at the abdominal part could be determined more accurately than at the central part of skipjack body. At the abdominal part, the SEP of 1.06% and 1.58% was achieved using the portable and desktop NIR spectrophotometers, respectively. In another work reported by Shimamoto et al. (2004), good agreements were also observed for fat content values measured by NIRS and wet chemical methods, with high R_C of 0.95 and 0.97 for frozen and thawed mackerel, respectively. Khodabux et al. (2007) proved the capability of NIRS (350–2500 nm) with the fiber optic probe for prediction of the total fat and free fat contents in tuna. The R_C of 0.95 and 0.96 was obtained in establishing the prediction models for total fat and free fat, respectively.

Prediction of fat content using RS. Unlike the extensive studies by NIRS technique, only few studies were reported on using RS to predict fat content in fish. First, in order to elucidate the potential of Raman spectra in measuring fat content of fish, Marquardt and Wold (2004) conducted an exploratory study in several species of intact fish fillets using RS (785 nm excitation) in tandem with a 25 × objective to collect the scattered radiation. Their results show that fish muscle exhibits little fluorescence at 785 nm excitation, thus exhibiting strong Raman scattering signals for fat analysis at approximately 1657, 1440, 1301 (CH_2 in phase twist), 1267(= C-H symmetric rock (*cis*)), 1076 (CCC stretch) and 1064 cm^{-1} (CCC stretch) (Sadeghi-Jorabchi et al., 1991; Howell et al., 2001). Further, Wold et al. (2004) investigated the feasibility of RS technique in quantifying the fat content of ground Atlantic salmon muscle by the aid of a spherical lens probe for efficient sampling. Good quantitative results were obtained in their work, with R_{CV} and SECV of 0.95 and 15.5 g/kg after spectral preprocessing and variable selection, which implies the high potential of RS technique in rapid prediction of fat content of fish.

Prediction of fat content using NMR. The ability of NMR technique to determine fat content of fish has already been investigated and significant correlations with chemical data were found. By using the low-field ^1H NMR operating at 23.2 MHz, an early study was reported by Jepsen et al. (1999) to predict fat content in intact salmon (*Salmo salar*). With the calibration model established by PLSR method, the independent test achieved an optimal SEP of 12 g/kg in fresh salmon flesh. Based on a self-calibrated NMR relaxometry method, Toussaint et al. (2002) conducted a study to determine the fat content of dried and homogenized brown trout (*Salmo trutta*) flesh. Their results showed that NMR technique gave an intermediate fat content value, 4.69% lower in relative value than those obtained by the Folch method and 6.75% higher than those by Soxhlet chemical extraction. Further, Veliyulin et al. (2005) employed a mobile LF-NMR spectrometer operating at 20 MHz (the *minispec* Bruker Professional Mouse) to quantify fat content and also visualize its distribution of the NQC of anaesthetized Atlantic salmon. Aside from achieving a good correlation ($R_C = 0.92$) between the reference fat values and those predicted by NMR, their work also gave a "fat image" for visualization of fat distribution, with a spatial resolution of about 5 mm, which allowed direct read-out of the fat value in any image pixel as well as the average fat content in a user-defined region of interest (ROI).

With the development of MRI technique, studies concerning prediction of fat content in fish have started to be reported. Brix et al. (2009) used a chemical shift based water-fat separation MRI technique for quantification and localization of fat in Atlantic mackerel, with the samples collected at three different nutritional stages. The authors succeeded in globally visualizing the fat, however, they did not find stable agreement between the fat content quantified by MRI and GC and could not clearly explain why. Afterwards, another study was conducted using the spin echo (SE) T1-weighted images, which is considered to attain high contrast between fat and muscle to measure the fat content in muscle and subcutaneous area of rainbow trout (*Oncorhynchus mykiss*) (Collewet et al., 2013). High correlations were obtained between the fat measured by MRI and GC techniques, with R_C^2 of 0.77 and 0.87 for the ventral and dorsal part, respectively.

Prediction of fat content using HSI. A range of studies has proved HSI to be a valid tool for fat analysis in fish. An early work was accomplished by ElMasry and Wold (2008), in which six species of fish fillets including Atlantic halibut, catfish, cod, mackerel, herring, and saithe were analyzed on-line by HSI to

obtain quantitative measurements of fat distribution. PLSR was undertaken to analyze the spectral data extracted from the corresponding hyperspectral images, followed by converting the pixel spectra to a distribution map of fat content. Their results showed that PLSR modeling method based on the spectral information between 760 and 1040 nm could yield a good prediction result for fat, with R_C and RMSECV of 0.91% and 2.99%, respectively. However, it needs to be noted that the reference fat values were measured by NMR technique in this work, which is not as classical and accurate as the traditional wet chemical method. Segtnan et al. (2009) carried out a work with an online NIR interactance imaging (760–1040 nm) to analyze the fat distribution in raw and salted salmon (*Salmo salar*) fillets. In this work, the instrument was calibrated using five cylindrical plugs (15 mm diameter) from each fillet. Their study showed good prediction results, with R_C and RMSECV of 0.95% and 1.96%, and 0.97% and 1.95% for raw fillets and salted fillets, respectively, which demonstrates that HSI is well suited for online assessment of chemical composition in fish. More recently, Zhu et al. (2014) applied another NIR HSI system with a wider spectral range of 899–1694 nm to determine the spatial distribution of fat in different positions of Atlantic salmon fillets. By extracting the mean spectrum from the ROI inside each hyperspectral image, and the quantitative relationship was developed, which gave the R_P and RMSEP of 0.93 and 1.24%, respectively. By applying the obtained quantitative model pixel-wise to the hyperspectral images, the chemical images of fat were produced in their work, which revealed that the fat content can vary greatly among different parts of salmon fish. Therefore, HSI technique makes it possible for fish manufacturers who wish to cut away fillets with certain threshold concentrations to perform it easily with limited modification in their production lines.

FAs composition

Prediction of FAs composition using NIRS. Free FAs (FFAs) are the hydrolytic products from fish lipid, and it has been recognized as a freshness index for a long time (Ke and Ackman, 1976). Using NIR transmittance spectra between 1100 and 2500 nm, an early study was conducted by Zhang and Lee (1997) to predict FFA content from the extracted fat of mackerel fish. They first established the calibration model using the artificially prepared samples, which were produced by adding different amounts of FFAs into commercial menhaden oil, and then the model was used to predict FFA content in mackerel fish stored at 4 and 24°C with different storage time. Both PLSR and MLR methods were applied to establish the prediction models, and by comparing the prediction results in commercial fish oil, PLSR model was selected to predict the FFA content in mackerel as producing less relative errors. For FFA in mackerel fat, the relative errors obtained were all less than 10%, which indicates the high potential of NIR transmittance spectra for prediction of FFA content in fish oil and therefore for the assessment of fish quality. Recently, another work was reported by Karlsdottir et al. (2014) on prediction of the FAs composition of two lean fish species, saithe, and hoki by direct application of the NIR reflectance fiber probe to the thawed and homogenized fish muscle samples. Based on the spectral information over the spectral range of 800–2500 nm and PLSR modeling method, the R_P^2, RMSEP and RPD of 0.98, 2.00 and 7.21, 0.96, 1.90, and 4.81, 0.93, 2.90, and 4.13 were obtained, respectively for prediction of total MUFAs, PUFAs, and FFAs in hoki samples, and 0.80, 1.35, and 2.84; 0.73, 0.81, and 1.98; and 0.83, 3.43, and 2.58, respectively, for saithe samples.

Regarding fish oil, it is only in the last decade that NIRS started to be applied extensively to measure its FAs. Using NIR spectra over the range of 2000–12,000 cm^{-1}, a study was conducted by Endo et al. (2005) to determine IV of eight species of fish oils, which consisted of salmon, sardine, tuna, cod, squid, orange roughy, myctophid, and stromateidei. By performing PLSR modeling method between the NIR absorbance spectra and the IV value measured by the titration method, they achieved the bias and the bias-corrected SEP of 0.00% and 1.3% for the whole set of the tested samples, which showed the excellence of NIRS for IV prediction in fish oils, with great accuracy and reproducibility. Another publication was found to evaluate the FFA content in fish oils using NIR transfelctance spectra (1100–2500 nm) (Cozzolino et al., 2005). Based on PLSR modeling method, satisfactory prediction result with R_P and SEP of 0.98 and 0.50 g/kg was achieved in their work. Later, Azizian et al. (2010) reported good agreement between the FT-NIR and GC measured values of individual FA content in fish oils. The determination coefficients were found to be high ($R_C^2 \geq 0.97$) for all the tested individual FA of C14:0, C16:0, C16:1 *cis*9, C18:0, C18:1 *cis*9, C18:2 *cis*9,*cis*12, C20:1 *cis*11, C18:3 *n*-3, C18:4 *n*-3, C20:4 *n*-3, C20:5 *n*-3, C22:5 *n*-3, and C22:6 *n*-3 in this work.

Studies have also been published on determination of the long chain *n*-3 FAs, such as EPA, DHA, and DPA in fish oils using NIRS. Bekhit et al. (2014) investigated the potential of NIRS (1100–2500 nm) in transflectance mode for prediction of the concentrations of EPA, DHA, and total *n*-3 FAs in fish oil supplements. The prediction models were established by PLSR method using the pre-processed spectra of the whole and selected regions, and the best prediction result was achieved with R_P^2 and SEP of 0.935% and 3.11%, 0.952% and 2.60%, and 0.996% and 1.60% for EPA, DHA, and total *n*-3 FAs, respectively. Another study was reported by Wu et al. (2014) using the Vis-short-wave NIR (Vis-SNIR) and long-wave NIR (LNIR) transmittance spectra to predict the content of EPA, DHA, and docosapentaenoic acid (DPA) in fish oils. Using the whole spectral information and the selected spectral variables by successive projections algorithm (SPA) and uninformative variable elimination (UVE), the quantitative models were established between the spectral data and reference PUFA contents based on PLSR algorithm. The best cross-validation results using the Vis-SNIR spectra were achieved with R_{CV}^2 and RMSECV of 0.942 and 16.07 mg/g, 0.903 and 10.93 mg/g, 0.905 and 1.84 mg/g for EPA, DHA, and DPA, respectively, and 0.944 and 15.77 mg/g, 0.908 and 10.61 mg/g, 0.979 and 0.85 mg/g, respectively, using the LNIR spectra.

Prediction of FAs composition using RS. Based on RS technique, a few studies have been carried out to characterize the FAs composition and IV of fish until recently, and its high potential has been proved. First, Afseth et al. (2005) evaluated the possibility of RS (785-nm laser) for FAs composition

determination in a complex food model system, which consisted of 70 different mixtures of protein, water, and oil blends in in order to create a rough chemical imitation of typical fish and meat samples. By performing PLSR method, they obtained the R_P and RMSEP of 0.99 and 6.8 g I_2/100 g fat, 0.99% and 2.9%, 0.95% and 3.9%, and 0.98% and 3.6% for prediction of IV and total SFAs, MUFAs, and PUFAs, respectively, which suggested the high potential of RS technique in prediction of FAs composition in real foods. Subsequently, by using RS equipped with the fiber optics to a Kaiser multireaction filtered probehead, Afseth et al. (2006) characterized the FAs composition and unsaturation of salmon in five sampling presentations, which consisted of oil extracts, ground samples and three types of intact samples collected from different positions according to NQC named as "Darkfat," "Skinfat" and "Infat" in their work. Based on PLSR modeling method, their results showed that Raman spectra collected from the oil extracts provided the most accurate IV prediction, with R_C and RMSECV of 0.87 and 2.5 g I_2/100 g fat, respectively. The R_C and RMSECV (g I_2/100 g fat) of ground salmon and intact cuts of "Darkfat," "Skinfat" and "Infat" achieved with 0.86 and 2.7, 0.73 and 3.5, and 0.80 and 3.1, 0.83, and 2.9, respectively. Higher prediction errors were obtained from Raman spectra of intact salmon muscle, which is considered to be partly owing to the sampling uncertainties in the relation between Raman measurements and reference analysis. More recently, Afseth et al. (2014) reported another study for qualitative and quantitative characterization of quality parameters of salmon through the skin by using s laboratory-based spatially offset RS (SORS) setup comprising an 830-nm laser. In this work, intact salmon samples with both dark and light skin were measured at different spatial offsets, and results showed that information regarding FAs composition could be obtained from both dark and light skin when using spatial offsets in the range of 5–6 mm, while conventional backscattering RS could not gain such information. By regressing the score values of the second principal component (PC) of Raman spectra to the GC measured IV values, they obtained high R_C^2 of 0.98 and 0.90 from the light and dark skin, respectively, which clearly reveal the quantitative potential of SORS spectra for through-skin analysis. However, only a small number of samples were covered in this study, and a large set of samples are still needed.

Regarding fish oil, Bekhit et al. (2014) reported the only work by applying RS technique to estimate the concentrations of EPA, DHA, and total *n*-3 FAs in fish oil supplements. In this work, the RS was equipped with an excitation wavelength of 785 nm and a fiber optic probe attached to a 20-cm-long immersion optic with a sapphire window at its tip for direct contact with sample surface. Using the whole and selected regions of polynomial curve-fitted and standard normal variate (SNV)-transformed Raman spectra, the best prediction result was achieved with R_P^2 and SEP of 0.961% and 2.73%, 0.947% and 2.56%, and 0.981% and 3.27%, respectively, for EPA, DHA and total *n*-3 FAs by performing PLSR modeling method.

Prediction of FAs composition using NMR. Based on NMR technique, many studies have been carried out to study its capability in predicting the FAs composition of fish and fish oil. Aursand and Grasdalen (1992) exploited the high-resolution ^{13}C NMR for FA analysis of lipid that extracted from the white muscle of Atlantic salmon (*Salmo salar*), and proved that the ^{13}C NMR spectra could provide information for analyzing FAs in fish. The authors found that in ^{13}C NMR spectrum, DHA has unique and well-resolved carbon resonances in the olefinic region originating from the C4 and C5 carbon, and also the *n*-3, *n*-6, *n*-7, and *n*-9/*n*-11 groups of FAs give rise to well-resolved signals in the spectrum which are unique for the respective groups. Aursand et al. (1993) applied the high-resolution ^{13}C NMR to define the *n*-3 FAs distribution in lipid extract and white muscle of Atlantic salmon (*Salmo salar*). Their results revealed that the ^{13}C spectrum of lipid extracted from fish muscle gaves quantitative information about the individual *n*-3 FAs, C18:2 *n*-6, C20:1/C22:1, and groups of FAs. In the ^{13}C NMR spectrum of white muscle, the methyl region of the acyl chains of triacylglycerols gave rise to sufficiently resolved signals to permit estimation of *n*-3 FAs content. Sacchi et al. (1993) also reported a good agreement between ^{1}H-NMR and GC determined *n*-3 PUFAs from fish lipids. Aursand et al. (1995) examined the positional distribution of *n*-3 FAs (C18:4 *n*-3, C20:4 *n*-3, C20:5 *n*-3, C22:5 *n*-3, and C22:6 *n*-3) in depot fat of Atlantic salmon (*Salmo salar*), harp seal oil, and cod liver oil triacylglycerols by ^{13}C NMR, and confirmed that ^{13}C NMR-derived data were in accordance with the corresponding data measured by conventional techniques.

Since the beginning of this century, the studies on using NMR technique to analyze the FAs composition of fish oil are increasing. Using a high-resolution proton ^{1}H NMR instrument performing at 300–500 MHz, two relevant studies were reported by Igarashi et al. (2000, 2002) to determine the concentration (mg/g) of DHA, the molar proportion (mol%) of DHA and the molar proportion of total *n*-3 FAs in fish oils. Four species of fish oils of bonito, tuna, and salmon and sardine oils were covered in their work, and the internal standard of ethylene glycol dimethyl ether (EGDM) was used mainly to allow quantification of DHA on a weight basis (mg/g). The RSD_r and RSD_R range of 0.91–2.62% and 1.73–4.27% was obtained, respectively for DHA concentration (mg/g), 0.59–3.46% and 0.23–0.90% for the molar proportion (mol%) of DHA, and 0.23–0.90% and 0.85–2.01% for total *n*-3 FAs. More recently, Wu et al. (2014) reported a work in which four potential spectroscopic techniques consisting of Vis-SNIR, LNIR, mid-infrared and NMR spectroscopy were compared with their performance in predicting EPA, DHA and DPA contents of fish oils. Their results showed that for the three studied PUFAs, the best predictions were all achieved by NMR technique, with the achieved R_{CV}^2 and RMSECV of 0.970 and 11.48 mg/g, 0.982 and 4.73 mg/g, and 0.983 and 0.77 mg/g, respectively for EPA, DHA, and DPA.

Regarding fish oil, apart from quantitative analysis of its FA contents, studies were also conducted for classification and authentication purposes. Based on the extracted fish oils from salmon muscle, Masoum et al. (2007) exploited the potential of ^{1}H NMR technique in combination with support vector machine (SVM) to classify wild and farmed salmon and their origins. The authors concluded that ^{1}H NMR spectra could provide useful information for analyzing FAs composition of

fish oils, and based on that, the wild and farmed salmon could be correctly distinguished, and ca. 5% misclassification rate of the country of origins was reported. For authentication purposes, Standal et al. (2009) carried out a study by applying ^{13}C NMR technique to distinguish different species of fish oils, which consisted of salmon, mackerel, and herring. Their results showed that significant differences exist in the sn-2 position specificity of C22:6 *n*-3, C20:5 *n*-3, and C18:4 *n*-3 among the species investigated. Also, the ^{13}C-NMR spectra in the carbonyl region exhibit clear distinction in their PCA clustering analysis, which makes it possible to distinguish these three fish oils solely from their ^{13}C-NMR spectra of carbonyl region. Also, some publications demonstrate that ^{13}C-NMR method is a promising technique for obtaining information about the positional distribution of FAs, especially EPA and DHA in fish oils (Aursand et al., 1995; Sacchi et al., 1994; Suárez et al., 2010; Tengku-Rozaina and Birch, 2014).

Conclusions and future trends

This review summarized the recent research progress of four nondestructive detection techniques, namely NIRS, RS, NMR, and HSI techniques in rapid determination of fat content and FAs composition of muscle foods, which consist of pork, beef, lamb, chicken meat, fish and fish oil. Overall, it can be seen that all the four techniques have been studied extensively for fat content and FAs composition analyses in muscle foods. Results published in different studies are variable and can be related to different influencing factors such as the instrument capabilities and settings, sample presentation, number of sample employed, statistical methods adopted and local conditions (industry or laboratory) among others.

In detail, NIRS technique was studied in the most extensive range among different varieties of muscle foods. NIRS has been applied to on-line prediction of fat content of ground meat under industrial condition, and satisfactory predictive performance was achieved. However, NIRS seems to have limited predictive capability for determining the fat content and FAs composition of intact meat, as the modeling results obtained were relatively low. The inferior performance of NIRS technique with intact meat is mainly due to that NIRS is based on point-detection, and such nature makes it difficult to cover the heterogeneous information of intact meat. The studies using RS, NMR, and HSI were relatively new and not extensive as NIRS; however, their great potential for analyzing fat content and FAs composition in different varieties of muscle foods has been proved. In particular, HSI fuses the merits of traditional imaging and spectroscopy techniques, and thus enables the mapping of fat/FAs within the tested sample, which is especially useful for non-homogeneous samples. As can be seen from the reported studies, HSI can achieve much better modeling results than NIRS for fat/FAs prediction in intact meat, which is mainly attributed to the mapping ability of HSI. However, there are still some challenges ahead for RS, NMR, and HSI techniques. Due to high dimensionality and time constraints for image acquisition and subsequent image analyses, seeking the most sensitive wavebands so that multispectral imaging systems can be built will be the trend in research and development of HSI technique.

Both RS and NMR remain expensive techniques now, and it is still far from introducing industrial Raman and NMR sensors on production lines in food factories. With the substantial development of hardware and software of the instrumental systems, the low-cost portable optical devices and fiber optic technique have appeared and are opening a new practical way for online analysis of food composition. In addition, as shown in the reported studies that the predictive accuracy for some FAs, especially minor amounts of FAs is not good yet and further improvement is still needed. Apart from the improvement and development of the hardware system, the information fusion of different techniques can also be a promising way for higher predictive accuracy.

References

Abeni, F. and Bergoglio, G. (2001). Characterization of different strains of broiler chicken by carcass measurements, chemical and physical parameters and NIRS on breast muscle. *Meat Sci.* **57**:133–137.

Afseth, N. K., Segtnan, V. H., Marquardt, B. J. and Wold, J. P. (2005). Raman and near-infrared spectroscopy for quantification of fat composition in a complex food model system. *Appl. Spectroscopy* **59** (11):1324–1332.

Afseth, N. K., Wold, J. P. and Segtnan, V. H. (2006). The potential of Raman spectroscopy for characterisation of the fatty acid unsaturation of salmon. *Anal. Chim. Acta* **572**:85–92.

Afseth, N. K., Bloomfield, M., Wold, J. P. and Matousek, P. (2014). A novel approach for subsurface through-skin analysis of salmon using spatially offset Raman spectroscopy (SORS). *Applied spectroscopy* **68**(2):255–262.

Aharoni, Y., Nachtomi, E., Hosltein, P., Brosh, A., Holzer, Z. and Nitsan, Z. (1995). Dietary effects on fat deposition and fatty acid profiles in muscle and fat depots of Friesian bull calves. *J. Anim. Sci.* **73**:2712–2720.

Alomar, D., Gallo, C., Castañeda, M. and Fuchslocher, R. (2003). Chemical and discriminant analysis of bovine meat by near infrared reflectance spectroscopy (NIRS). *Meat Sci.* **63**:441–450.

Anderson, N. M. and Walker, P. N. (2003). Measuring fat content of ground beef stream using on-line visible/NIR spectroscopy. *Trans. ASAE* **46**(1):117–124.

Andres, S., Murray, I., Navajas, E. A., Fisher, A. V., Lambe, N. R. and Bunger, L. (2007). Prediction of sensory characteristics of lamb meat samples by near infrared reflectance spectroscopy. *Meat Sci.* **76**:509–516.

Aursand, M. and Grasdalen, H. (1992). Interpretation of the ^{13}C NMR spectra of omega-3 fatty acids and lipid extracted from the white muscle of Atlantic salmon (Salmo salar). *Chem. Phys. Lipids* **62**:239–251.

Aursand, M., Rainuzzo, J. R. and Grasdalen, H. (1993). Quantitative high-resolution ^{13}C and ^{1}H nuclear magnetic resonance of ω-3 fatty acids from white muscle of atlantic salmon (Salmo salar). *J. Am. Oil Chem. Soc.* **70**:971–981.

Aursand, M., Jorgensen, L. and Grasdalen, H. (1995). Positional distribution of ω-3 fatty acids in marine lipid triacylglycerols by high-resolution ^{13}C nuclear magnetic resonance spectroscopy. *J. Am. Oil Chem. Soc.* **72**(3):293–297.

Aursand, I.G., Veliyulin, E. and Erikson, U. (2006). Low-field NMR studies of Atlantic salmon (*Salmo salar*). Springer: Modern Magnetic Resonance:905–913.

Azizian, H., Kramer, J. K. G., Ehler, S. and Curtis, J. M. (2010). Rapid quantitation of fish oil fatty acids and their ethyl esters by FT-NIR models. *Eur. J. Lipid Sci. Technol.* **112**:452–462.

Baeten, V., Meurens, M., Morales, M. T. and Aparicio, R. (1996). Detection of virgin olive oil by Fourier transform Raman spectroscopy. *J. Agric. Food Chem.* **44**:2225–2230.

Balage, J. M., Silva, S. da L. e, Gomide, C. A., Bonin, M. de N. and Figueira, A. C. (2015). Predicting pork quality using Vis/NIR spectroscopy. *Meat Sci.* **108**:37–43.

Ballerini, L., Hogberg, A., Borgefors, G., Bylund, A. C., Lindgard, A., Lundstrom, K., et al. (2002). A segmentation technique to determine fat content in NMR images of beef meat. *IEEE Trans. Nucl. Sci.* **49**(1):195–199.

Barbin, D. F., ElMasry, G., Sun, D.-W., and Allen, P. (2013). Non-destructive determination of chemical composition in intact and minced pork using near-infrared hyperspectral imaging. *Food Chem.* **138**:1162–1171.

Barlocco, N., Vadell, A., Ballesteros, F., Galietta, G. and Cozzolino, D. (2006). Predicting intramuscular fat, moisture and Warner-Bratzler shear force in pork muscle using near infrared reflectance spectroscopy. *Animal Sci.* **82**:111–116.

Bauchart, D., Roy, A., Lorenz, S., Chardigny, J. M., Ferlay, A., Gruffat, D., et al. (2007). Butters varying in *trans* 18:1 and *cis*-9, *trans*-11 conjugated linoleic acid modify plasma lipoproteins in the hypercholesterolemic rabbit. *Lipids* **42**:123–133.

Beattie, R. J., Bell, S. J., Farmer, L. J., Moss, B. W. and Desmond, P. D. (2004). Preliminary investigation of the application of Raman spectroscopy to the prediction of the sensory quality of beef silverside. *Meat Sci.* **66**:903–913.

Beattie, J. R., Bell, S. E. J., Borgaard, C., Fearon, A. and Moss, B. W. (2006). Prediction of adipose tissue composition using Raman spectroscopy: Average properties and individual fatty acids. *Lipids* **41**(3):287–294.

Beattie, J. R., Bell, S. E. J., Borggaard, C., Fearon, A. M. and Moss, B. W. (2007). Classification of adipose tissue species using raman spectroscopy. *Lipids* **42**:679–685.

Bekhit, M. Y., Grung, B. and Mjøsa, S. A. (2014). Determination of omega-3 fatty acids in fish oil supplements using vibrational spectroscopy and chemometric methods. *Appl. Spectros.* **68**(10):1190–1200.

Berhe, D. T., Eskildsen, C. E., Lametsch, R., Hviid, M. S., van den Berg, F. and Engelsen, S. B. (2016). Prediction of total fatty acid parameters and individual fatty acids in pork backfat using Raman spectroscopy and chemometrics: Understanding the cage of covariance between highly correlated fat parameters. *Meat Sci.* **111**:18–26.

Berzaghi, P., Dalle Zotte, A., Jansson, L. M. and Andrighetto, I. (2005). Near-infrared reflectance spectroscopy as a method to predict chemical composition of breast meat and discriminate between different *n*-3 feeding sources. *Poultry Sci.* **84**:128–136.

Bloch, F., Hansen, W. W. and Packard, M. (1946). Nuclear induction. *Phys. Rev.* **69**:127–127.

Bosch, L., Tor, M., Reixach, J. and Estany, J. (2012). Age-related changes in intramuscular and subcutaneous fat content and fatty acid composition in growing pigs using longitudinal data. *Meat Sci.* **91**(3):358–363.

Boyaci, I. H., Uysal, R. S., Temiz, T., Shendi, E. G., Yadegari, R. J., Rishkan, M. M., Velioglu, H. M., Tamer, U., Ozay, D. S. and Vural, H. (2014). A rapid method for determination of the origin of meat and meat products based on the extracted fat spectra by using of Raman spectroscopy and chemometric method. *Eur. Food Res. Technol.* **238**:845–852.

Bressan, M. C., Rossato, L. V., Rodrigues, E. C., Alves, S. P., Bessa, R. J. B., Ramos, E. M. and Gama, L. T. (2011). Genotype×environment interactions for fatty acids profiles in *Bos indicus* and *Bos taurus* finished on pasture or grain. *J. Anim. Sci.* **89**:221–232.

Brix, O., Apablaza, P., Baker, A., Taxt, T. and Gruner, R. (2009). Chemical shift based MR imaging and gas chromatography for quantification and localization of fat in Atlantic mackerel. *J. Expe. Mar. Biol. Ecology* **376**(2):68–75.

Brøndum, J., Munck, L., Henckel, P., Karlsson, A., Tornberg, E. and Engelsen, S. B. (2000). Prediction of water-holding capacity and composition of porcine meat by comparative spectroscopy. *Meat Sci.* **55**:177–185.

Brown, M. R., Kube, P. D., Taylor, R. S. and Elliott, N. G. (2014). Rapid compositional analysis of Atlantic salmon (Salmo salar) using visible-near infrared reflectance spectroscopy. *Aquaculture Res.* **45**:798–811.

Burns, D. A. and Ciurczak, E. W. (Eds.). (2001). *Handbook of Near-infrared Analysis*, Revised and Expanded, 2nd ed., Marcel Dekker, Inc., New York, Basel, Hingkong.

Cecchinato, A., Marchi, M. De, Penasa, M., Casellas, J., Schiavon, S. and Bittante, G. (2012). Genetic analysis of beef fatty acid composition predicted by near-infrared spectroscopy. *J. Anim. Sci.* **90**(2):429–438.

Cen, H. and He, Y. (2007). Theory and application of near infrared reflectance spectroscopy in determination of food quality. *Trends Food Sci Technol* **18**(2):72–83.

Chan, D. E., Walker, P. N. and Mills, E. W. (2002). Prediction of pork quality characteristics using visible and near-infrared spectroscopy. *Trans. ASAE* **45**:1519–1527.

Collewet, G., Bugeon, J., Idier, J., Quellec, S., Quittet, B., Cambert, M. and Haffray, P. (2013). Rapid quantification of muscle fat content and subcutaneous adipose tissue in fish using MRI. *Food Chem.* **138**(2–3):2008–2015.

Combe, N., Clouet, P., Chardigny, J. M., Lagarde, M. and Léger, C. L. (2007). *Trans* fatty acids, conjugated linoleic acids, and cardiovascular diseases. *Eur. J. Lipid Sci. Technol.* **109**:945–953.

Correa, J., Faucitano, L., Laforest, J., Rivest, J., Marcoux, M. and Garíepy, C. (2006). Effects of slaughter weight on carcass composition and meat quality in pigs of two different growth rates. *Meat Sci.* **72**(1):91–99.

Cozzolino, D., Murray, I. and Paterson, R. (1996). Visible and near infrared reflectance spectroscopy for the determination of moisture, fat and protein in chicken breast and thigh muscle. *J. Near Infrared Spectrosc.* **4**(1):213–223.

Cozzolino, D. and Murray, I. (2002). Effect of sample presentation and animal muscle species on the analysis of meat by near infrared reflectance spectroscopy. *J. Near Infrared Spectrosc.* **10**:37–44.

Cozzolino, D., De Mattos, D. and Martins, V. (2002). Visible/near infrared reflectance spectroscopy for predicting composition and tracing system of production of beef muscle. *Animal Sci.* **74**:477–484.

Cozzolino, D., Murray, I., Chree, A. and Scaife, J. R. (2005). Multivariate determination of free fatty acids and moisture in fish oils by partial least-squares regression and near-infrared spectroscopy. *LWT-Food Sci. Technol.* **38**:821–828.

De Marchi, M., Riovanto, R., Penasa, M. and Cassandro, M. (2012). At-line prediction of fatty acid profile in chicken breast using near infrared reflectance spectroscopy. *Meat Sci.* **90**:653–657.

De Pedro, E., Núñez, N., García, J., Aparicio, D., Campos, M. I., Pérez, M. D., Fernández, V. M. and Garrido, A. (2007). Implementing near infrared spectroscopy in the Iberian pig industry. *Options Méditerranéennes* **76**:225–228.

Duda, M. K., O'Shea, K. M. and Stanley, W. C. (2009). Omega-3 polyunsaturated fatty acid supplementation for the treatment of heart failure: Mechanisms and clinical potential. A *review*. *Cardiovasc. Res.* **84**(1):33–41.

ElMasry, G. and Wold, J. P. (2008). High-speed assessment of fat and water content distribution in fish fillets using online imaging spectroscopy. *J. Agric. Food Chem.* **56**:7672–7677.

ElMasry, G., Barbin, D. F., Sun, D.-W. and Allen, P. (2012). Meat quality evaluation by hyperspectral imaging technique: an overview. *Crit. Rev. Food Sci. Nutr.* **52**(8):689–711.

ElMasry, G., Sun, D.-W. and Allen, P. (2013). Chemical-free assessment and mapping of major constituents in beef using hyperspectral imaging. *Journal of Food Engineering* **117**:235–246.

Emerson, M. R., Woerner, D. R., Belk, K. E. and Tatum, J. D. (2013). Effectiveness of USDA instrument-based marbling measurements for categorizing beef carcasses according to differences in longissimus muscle sensory attributes. *J.f Animal Sci.* **91**(2):1024–1034.

Endo, Y., Tagiri-Endo, M. and Kimura, K. (2005). Rapid determination of iodine value and saponification value of fish oils by near-infrared spectroscopy. *J. Food Sci.* **70**(2):C127–C131.

Fernandez, X., Monin, G., Talmant, A., Mourot, J. and Lebret, B. (1999a). Influence of intramuscular fat content on the quality of pig meat −2. Consumer acceptability of *m. longissimus lumborum*. *Meat Sci.* **53**:67–72.

Fernandez, X., Monin, G., Talmant, A., Mourot, J. and Lebret, B. (1999b). Influence of intramuscular fat content on the quality of pig meat −1. Composition of the lipid fraction and sensory characteristics of *m. longissimus lumborum*. *Meat Sci.* **53**(1):59–65.

Folkestad, A., Wold, J. P., Rørvik, K.-A., Tschudi, J., Haugholt, K. H., Kolstad, K. and Mørkøre, T. (2008). Rapid and non-invasive measurements of fat and pigment concentrations in live and slaughtered Atlantic salmon (*Salmo salar* L.). *Aquaculture* **280**:129–135.

Fowler, S. M., Ponnampalam, E. N., Schmidt, H., Wynn, P. and Hopkins, D. L. (2015). Prediction of intramuscular fat content and major fatty acid groups of lamb M. *longissimus lumborum using Raman spectroscopy*. *Meat Sci.* **110**:70–75.

Gjerde, B. and Martens, H. (1987). Predicting carcass composition of rainbow trout by near-infrared spectroscopy. *J. Anim. Breed. Genet.* **104**:137–148.

Gjerlaug-Enger, E., Kongsro, J., Aass, L., Odegård, J. and Vangen, O. (2011). Prediction of fat quality in pig carcasses by near-infrared spectroscopy. *Animal* **5**(11):1829–1841.

Goetz, A. F. H., Vane, G., Solomon, J. E. and Rock, B. N. (1985). Imaging spectrometry for earth remote sensing. *Science* **228**:1147–1153.

González-Martín, I., González-Pérez, C., Hernández-Méndez, J., Álvarez-García, N. and Lázaro, S. M. (2002). Determination of fatty acids in subcutaneous fat of Iberian breed swine by near infrared spectroscopy. A comparative study of the methods for obtaining total lipids: solvents and melting with microwaves. *J. Near Infrared Spectrosc.* **10**:257–268.

González-Martín, I., González-Pérez, C., Hernández-Méndez, J. and álvarez-García, N. (2003). Determination of fatty acids in the subcutaneous fat of Iberian breed swine by near infrared spectroscopy (NIRS) with a fibre-optic probe. *Meat Sci.* **65**:713–719.

González-Martín, I., Gonzáles-Pérez, C., Alvarez-García, N. and Gonzáles-Cabrera, J. M. (2005). On-line determination of fatty acid composition in intramuscular fat of Iberian pork loin by NIRS with a remote reflectance fibre optic probe. *Meat Sci.* **69**:243–248.

Gutowsky, H. S., Kistiakowsky, G. B., Pake, G. E. and Purcell, E. M. (1949). Structural investigations by means of nuclear magnetism. 1. Rigid crystal lattices. *J. Chem. Phys.* **17**(10):972–981.

Guy, F., Prache, S., Thomas, A., Bauchart, D. and Andueza, D. (2011). Prediction of lamb meat fatty acid composition using near-infrared reflectance spectroscopy (NIRS). *Food Chem.* **127**:1280–1286.

Hayes, K. C. and Khosla, D. R. (1992). Dietary fatty acids thresholds and cholesterolemia. *FASEB J.* **6**:2600–2607.

Herdmann, A., Martin, J., Nuernberg, G., Wegner, J., Dannenberger, D. and Nuernberg, K. (2010). How do *n*-3 fatty acid (short time restricted *vs* unrestricted) and *n*-6 fatty acid enriched diets affect the fatty acid profile in different tissues of German Simmental bulls? *Meat Sci.* **86**:712–719.

Hoving-Bolink, A. H., Vedder, H. W., Merks, J. W. M., de Klein, W. J. H., Reimert, H. G. M., Frankhuizen, R., van den Broekb, W. H. A. M. and Lambooija, en E. (2005). Perspective of NIRS measurements early post-mortem for prediction of pork quality. *Meat Sci.* **69**(3):417–423.

Howell, N. K., Herman, H. and Li-Chan, E. C. Y. (2001). Elucidation of protein-lipid interactions in a lysozyme-corn oil system by Fourier transform Raman spectroscopy. *J. Agric. Food Chem.* **49**:1529–1533.

Hu, F. B., Stampfer, M. J., Manson, J. A. E., Ascherio, A., Colditz, G. A., Speizer, F. E., Hennekens, C. H and Willett, W. C. (1999). Dietary saturated fats and their food sources in relation to the risk of coronary heart disease in women. *Am. J. Clin. Nutrition* **70**:1001–1008.

Hu, Y., Guo, K., Suzuki, T., Noguchi, G. and Satake, T. (2008). Quality evaluation of fresh pork using visible and near-infrared spectroscopy with fiber optics in interactance mode. *Trans. ASABE* **51**(3):1029–1033.

Huang, H., Liu, L., Ngadi, M. O. and Gariépy, C. (2013). Prediction of pork marbling scores using pattern analysis techniques. *Food Control* **31**(1):224–229.

Huang, H., Liu, L., Ngadi, M. O., Gariépy, C. and Prasher, S. O. (2014a). Near-infrared spectral image analysis of pork marbling based on gabor filter and wide line detector techniques. *Appl. Spectrosc.* **68**(3):332–339.

Huang, H., Liu, L., Ngadi, M. O. and Gariépy, C. (2014b). Rapid and non-invasive quantification of intramuscular fat content of intact pork cuts. *Talanta* **119**:385–395.

Igarashi, T., Aursand, M., Hirata, Y., Gribbestad, I. S., Wada, S. and Nonaka, M. (2000). Nondestructive quantitative determination of docosahexaenoic acid and *n*-3 fatty acids in fish oils by high-resolution ^{1}H nuclear magnetic resonance spectroscopy. *JAOCS* **77**:737–748.

Igarashi, T., Aursand, M., Sacchi, R., Paolillo, L., Nonaka, M. and Wada, S. (2002). Determination of docosahexaenoic acid and *n*-3 fatty acids in refined fish oils by 1H-NMR spectroscopy: IUPAC interlaboratory study. *JAOAC Int.* **85**(6):1341–1354.

Isaksson, T., Tøgersen, G., Iversen, A. and Hildrum, K. I. (1995). Nondestructive determination of fat, moisture and protein in salmon fillets by use of near infrared diffuse spectroscopy. *J. Sci. Food Agric.* **69**:95–100.

Jahan, K., Paterson, A. and Spickett, C. M. (2004). Fatty acid composition, antioxidants and lipid oxidation in chicken breasts from different production regimes. *Int. J. Food Sci. Technol.* **39**:443–453.

Jepsen, S. M., Pedersen, H. T. and Engelsen, S. B. (1999). Application of chemometrics to low-field ^{1}H NMR relaxation data of intact fish flesh. *J. Sci. Food Agric.* **79**:1793–1802.

Kamruzzaman, M., ElMasry, G., Sun, D.-W. and Allen, P. (2012). Non-destructive prediction and visualization of chemical composition in lamb meat using NIR hyperspectral imaging and multivariate regression. *Innovative Food Sci. Emerging Technol.* **16**:218–226.

Karlsdottir, M. G., Arason, S., Kristinsson, H. G. and Sveinsdottir, K. (2014). The application of near infrared spectroscopy to study lipid characteristics and deterioration of frozen lean fish muscles. *Food Chem.* **159**:420–427.

Ke, P. J. and Ackman, R. G. (1976). Metal-catalyzed oxidation in mackerel skin and meat lipids. *J. Am. Oil Chem. Soc.* **53**:636–640.

Keeton, J. T., Hafley, B. S., Eddy, S. M., Moser, C. R., McManus, B. J. and Leffler, T. P. (2003). Rapid determination of moisture and fat in meats by microwave and nuclear magnetic resonance analysis-PVM 1:2003. *J. AOAC Int.* **86**(6):1193–1202.

Khodabux, K., L'Omelette, M. S. S., Jhaumeer-Laulloo, S., Ramasami, P. and Rondeau, P. (2007). Chemical and near-infrared determination of moisture, fat and protein in tuna fishes. *Food Chem.* **102**:669–675.

Kobayashi, K.-I., Matsui, Y., Maebuchi, Y., Toyota, T. and Nakauchi, S. (2010). Near infrared spectroscopy and hyperspectral imaging for prediction and visualisation of fat and fatty acid content in intact raw beef cuts. *J. Near Infrared Spectrosc.* **18**:301–315.

Kövér, G., Romvári, R., Horn, P., Berényi, E., Jensen, J. F. and Sørensen, P. (1998). In vivo assessment of breast muscle, abdominal fat and total fat volume in meat-type chickens by magnetic resonance imaging. *Acta Vet Hung* **46**(2):135–144.

Kratz, M., Baars, T. and Guyenet, S. (2013). The relationship between high-fat dairy consumption and obesity, cardiovascular, and metabolic disease. *Eur. J. Nutrition* **52**:1–24.

Lanza, E. (1983). Determination of moisture, protein, fat and calories in raw pork and beef by near infrared spectroscopy. *J. Food Sci.* **48**:471–474.

Lee, S., Lohumi, S., Lim, H.-S., Gotoh, T., Cho, B.-K. and Jung, S. (2015). Determination of Intramuscular Fat Content in Beef using Magnetic Resonance Imaging. *J. Fac. Agr., Kyushu Univ.* **60** (1):157–162.

Leffler, T. P., Moser, C. R., McManus, B. J., Urh, J. J., Keeton, J. T., and Claflin, A. (2008). Determination of moisture and fat in meats by microwave and nuclear magnetic resonance analysis: Collaborative study. *J. AOAC Int.* **91**(4):802–810.

Li-Chan, E. C. Y. (1996). The applications of Raman spectroscopy in food science. *Trends Food Sci. Technol.* **7**:361–370.

Link, B. A., Bray, R. W., Cassens, R. G. and Kauffman, R. G. (1970). Fatty acid composition of bovine skeletal muscle lipids during growth. *J. Anim. Sci.* **30**:726–731.

Liu, L., Ngadi, M. O., Prasher, S. O. and Gariépy, C. (2012). Objective determination of pork marbling scores using the wide line detector. *J. Food Eng.* **110**(3):497–504.

Liu, L. and Ngadi, M. O. (2014). Predicting intramuscular fat content of pork using hyperspectral imaging. *J. Food Eng.* **134**:16–23.

Lohumi, S., Lee, S., Lee, H., Kim, M. S., Lee, W.-H. and Cho, B.-K. (2016). Application of hyperspectral imaging for characterization of intramuscular fat distribution in beef. *Infrared Phys. Technol.* **74**:1–10.

Lyndgaard, L. B., Sørensen, K. M., van den Berg, F. and Engelsen, S. B. (2012). Depth profiling of porcine adipose tissue by Raman spectroscopy. *J. Raman Spectrosc.* **43**:482–489.

Måge, I., Wold, J. P., Bjerke, F. and Segtnan, V. (2013). On-line sorting of meat trimmings into targeted fat categories. *J. Food Eng.* **115**:306–313.

Malau-Aduli, A. E. O., Siebert, B. D., Bottema, C. D. K. and Pitchford, W. S. (1998). Breed comparison of the fatty acid composition of muscle phospholipids in Jersey and Limousin cattle. *J. Anim. Sci.* **76**:766–773.

Maltin, C. A., Sinclair, K. D., Warris, P. D., Grant, C. M., Porter, A. D., Delday, M. I. and Warkup, C. C. (1998). The effects of age at slaughter, genotype and finishing system on the biochemical properties, muscle fibre type characteristics and eating quality of bull beef from suckled calves. *Anim. Sci.* **66**:341–348.

Marcone, M. F., Wang, S., Albabish, W., Nie, S., Somnarain, D. and Hill, A. (2013). Diverse food-based applications of nuclear magnetic resonance (NMR) technology. *Food Res. Int.* **51**:729–747.

Maria, R. M., Colnago, L. A., Forato, L. A. and Bouchard, D. (2010). Fast and simple nuclear magnetic resonance method to measure conjugated linoleic acid in beef. *J. Agric. Food Chem.* **58**(11):6562–6564.

Marquardt, B. J. and Wold, J. P. (2004). Raman analysis of fish:a potential method for rapid quality screening. *Lebensm.-Wiss. u.-Technol.* **37**:1–8.

Masoum, S., Malabat, C., Jalali-Heravi, M., Guillou, C., Rezzi, S. and Rutledge, D. N. (2007). Application of support vector machines to ^{1}H NMR data of fish oils: methodology for the confirmation of wild and farmed salmon and their origins. *Anal. Bioanal Chem.* **387**:1499–1510.

Mazurek, S., Szostak, R., Czaja, T. and A., Zachwieja. (2015). Analysis of milk by FT-Raman spectroscopy. *Talanta* **138**:285–289.

McDevitt, R. M., Gavin, A. J., Andrés, S. and Murray, I. (2005). The ability of visible and near infrared reflectance spectroscopy to predict the chemical composition of ground chicken carcasses and to discriminate between carcasses from different genotypes. *J. Near Infrared Spectrosc.* **13**(3):109–117.

Mitchell, A. D., Rosebrough, R. W., Taicher, G. Z. and Kovner, I. (2011). In vivo measurement of body composition of chickens using quantitative magnetic resonance. *Poultry Sci.* **90**:1712–1719.

Monziols, M., Collewet, G., Mariette, F., Kouba, M. and Davenel, A. (2005). Muscle and fat quantification in MRI gradient echo images using a partial volume detection method. Application to the characterization of pig belly tissue. *Magn. Reson. Imaging* **23**:745–755.

Monziols, M., Collewet, G., Bonneau, M., Mariette, F., Davenel, A. and Kouba, M. (2006). Quantification of muscle, subcutaneous fat and intermuscular fat in pig carcasses and cuts by magnetic resonance imaging. *Meat Sci.* **72**:146–154.

Morlein, D., Rosner, F., Brand, S., Jenderka, K.-V. and Wicke, M. (2005). Non-destructive estimation of the intramuscular fat content of the longissimus muscle of pigs by means of spectral analysis of ultrasound echo signals. *Meat Sci.* **69**(2):187–199.

Motoyama, M., Ando, M., Sasaki, K. and Hamaguchi, H.-O. (2010). Differentiation of Animal Fats from Different Origins: Use of Polymorphic Features Detected by Raman Spectroscopy. *Appl. Spectrosc.* **64** (11):1244–1250.

Mourot, B. P., Gruffat, D., Durand, D., Chesneau, G., Prache, S., Mairesse, G. and Andueza, D. (2014). New approach to improve the calibration of main fatty acids by near-infrared reflectance spectroscopy in ruminant meat. *Animal Prod. Sci.* **54**:1848–1852.

Müller, M. and Scheeder, M. R. L. (2008). Determination of fatty acid composition and consistency of raw pig fat with near infrared spectroscopy. *J Near Infrared Spectrosc.* **16**(3):305–309.

Murphy, K. J., Meyer, B. J., Mori, T. A., Burke, V., Mansour, J., Patch, C. S., et al. (2007). Impact of foods enriched with n-3 long-chain polyunsaturated fatty acids on erythrocyte *n*-3 levels and cardiovascular risk factors. *Br. J. Nutr.* **97**:749–757.

Murray, I. and Williams, P. C. (1987). Chemical principles of Near infrared technology in the agricultural and food industries, Ed by P. Williams and K. H. Norris. American Association of Cereal Chemists, St Paul, MN, USA, p. 17.

Nakashima, Y. (2015). Development of a single-sided nuclear magnetic resonance scanner for the in vivo quantification of live cattle marbling. *Appl. Magn. Reson.* **46**:593–606.

Nicolai, B. M., Beullens, K., Bobelyn, E., Peirs, A., Saeys, W., Theron, K. I. and Lammertyn, J. (2007). Nondestructive measurement of fruit and vegetable quality by means of NIR spectroscopy: A review. *Postharvest Biol. Technol.* **46**(2):99–118.

Noci, F., French, P., Monahan, F. J. and Maloney, A. P. (2007). The fatty acid composition of muscle fat and subcutaneous adipose tissue of grazing heifers supplemented with plant oil-enriched concentrates. *J. Anim. Sci.* **85**:1062–1073.

Nogi, T., Honda, T., Mukai, F., Okagaki, T. and Oyama, K. (2011). Heritabilities and genetic correlations of fatty acid compositions in longissimus muscle lipid with carcass traits in Japanese Black cattle. *J. Anim. Sci.* **89**:615–621.

Nortvedt, R., Torrissen, O. J. and Tuene, S. (1998). Application of near-infrared transmittance spectroscopy in the determination of fat, protein and dry matter in Atlantic halibut fillet. *Chemometr. Intell. Lab. Syst.* **42**:199–207.

Oka, A., Iwaki, F., Dohgo, T., Ohtagaki, S., Noda, M., Shiozaki, T., Endoh, O. and Ozaki, M. (2002). Genetic effects on fatty acid composition of carcass fat of Japanese Black Wagyu steers. *J. Anim. Sci.* **80**:1005–1011.

Olivares, A., Daza, A., Rey, A. and Lopez-Bote, C. (2009). Interactions between genotype, dietary fat saturation and vitamin A concentration on intramuscular fat content and fatty acid composition in pigs. *Meat Sci.* **82**(1):6–12.

Olsen, E. F., Rukke, E. O., Flatten, A. and Isaksson, T. (2007). Quantitative determination of saturated-, monounsaturated- and polyunsaturated fatty acids in pork adipose tissue with non-destructive Raman spectroscopy. *Meat Sci.* **76**:628–634.

Olsen, E. F., Rukke, E. O., Egelandsdal, B. and Isaksson, T. (2008). Determination of omega-6 and omega-3 fatty acids in pork adipose tissue with nondestructive Raman and fourier transform infrared spectroscopy. *Appl. Spectrosc.* **62**(9):968–974.

Olsen, E. F., Baustad, C., Egelandsdal, B., Rukke, E.-O. and Isaksson, T. (2010). Long-term stability of a Raman instrument determining iodine value in pork adipose tissue. *Meat Sci.* **85**:1–6.

Ozaki, Y., Cho, R., Ikegaya, S., Muraishi, S. and Kawauchi, K. (1992). Potential of near-infrared Fourier transform Raman spectroscopy in food analysis. *Appl. Spectrosc.* **46**:1503–1507.

Pérez-Juan, M., Afseth, N. K., González, J., Díaz, I., Gispert, M., Font i Furnols, M., Oliver, M. A. and Realini, C. E. (2010). Prediction of fatty acid composition using a NIRS fibre optics probe at two different locations of ham subcutaneous fat. *Food Res. Int.* **43**:1416–1422.

Pérez-Marín, D., De Pedro Sanz, E., Guerrero-Ginel, J. E. and Garrido-Varo, A. (2009). A feasibility study on the use of near-infrared spectroscopy for prediction of the fatty acid profile in live Iberian pigs and carcasses. *Meat Sci.* **83**:627–633.

Perry, D., Nicholls, P. J. and Thompson, J. M. (1998). The effect of sire breed on the melting point and fatty acid composition of subcutaneous fat in steers. *J. Anim. Sci.* **76**:87–95.

Pitchford, W. S., Deland, M. P. B., Siebert, B. D., Malau-Aduli, A. E. O. and Bottema, C. D. K. (2002). Genetic variation in fatness and fatty acid composition of crossbred cattle. *J. Anim. Sci.* **80**:2825–2832.

Platter, W. J., Tatum, J. D., Belk, K. E., Chapman, P. L., Scanga, J. A. and Smith, G. C. (2003). Relationships of consumer sensory ratings, marbling score, and shear force value to consumer acceptance of beef strip loin steaks. *J. Anim. Sci.* **81**:2741–2750.

Prema, D., Turner, T. D., Jensen, J., Pilfold, J. L., Church, J. S., Donkor, K. K. and B. Cinel. (2015). Rapid determination of total conjugated linoleic acid concentrations in beef by ^{1}H NMR spectroscopy. *J. Food Compos. Anal.* **41**:54–57.

Prevolnik, M., Candek-Potokar, M. and Skorjanc, D. (2004). Ability of NIR spectroscopy to predict meat chemical composition and quality-a review. *Czech J. Animal Sci.* **49**(11):500–510.

Prieto, N., Andrés, S., Giráldez, F. J., Mantecón, A. R. and Lavín, P. (2006). Potential use of near infrared reflectance spectroscopy (NIRS) for the estimation of chemical composition of oxen meat samples. *Meat Sci.* **74**:487–496.

Prieto, N., Ross, D. W., Navajas, E. A., Richardson, R. I., Hyslop, J. J., Simm, G. and Roehe, R. (2011). Online prediction of fatty acid profiles in crossbred Limousin and Aberdeen Angus beef cattle using near infrared reflectance spectroscopy. *Animal* **5**(1):155–165.

Prieto, N., Dugan, M. E. R., López-Campos, O., McAllister, T. A., Aalhus, J. L. and Uttaro, B. (2012). Near infrared reflectance spectroscopy predicts the content of polyunsaturated fatty acids and biohydrogenation products in the subcutaneous fat of beef cows fed flaxseed. *Meat Sci.* **90**:43–51.

Prieto, N., Dugan, M. E. R., López-Campos, Ó., Aalhus, J. L. and Uttaro, B. (2013). At line prediction of PUFA and biohydrogenation intermediates in perirenal and subcutaneous fat from cattle fed sunflower or flaxseed by near infrared spectroscopy. *Meat Sci.* **94**:27–33.

Prieto, N., Uttaro, B., Mapiye, C., Turner, T. D., Dugan, M. E. R., Zamora, V., Young, M. and Beltranena, E. (2014). Predicting fat quality from pigs fed reduced-oil corn dried distillers grains with solubles by near infrared reflectance spectroscopy: Fatty acid composition and iodine value. *Meat Sci.* **98**:585–590.

Pullanagari, R. R., Yule, I. J. and Agnew, M. (2015). On-line prediction of lamb fatty acid composition by visible near infrared spectroscopy. *Meat Sci.* **100**:156–163.

Purcell, E. M., Torrey, H. C. and Pound, R. V. (1946). Resonance absorption by nuclear magnetic moments in a solid. *Phys. Rev.* **69**(1–2):37–38.

Qiao, J., Ngadi, M. O., Wang, N., Gariépy, C. and Prasher, S.O. (2007). Pork quality and marbling level assessment using a hyperspectral imaging system. *J. Food Eng.* **83**(1):10–16.

Raman, C. V. and Krishnan, K. S. (1928). A new type of secondary radiation. *Nature* **121**(3048):501–502.

Realini, C. E., Duckett, S. K. and Windham, W. R. (2004). Effect of vitamin C addition to ground beef from grass-fed or grain-fed sources on color and lipid stability, and prediction of fatty acid composition by near-infrared reflectance analysis. *Meat Sci.* **68**:35–43.

Renden, J. A., Oates, S. S. and Reed, R. B. (1986). Determination of body fat and moisture in dwarf hens with near-infrared reflectance spectroscopy. *Poultry Sci.* **65**:1539–1541.

Ripoche, A. and Guillard, A. S. (2001). Determination of fatty acid composition of pork fat by Fourier transdform infrared spectroscopy. *Meat Sci.* **58**:299–304.

Ripoll, G., Alberti, P., Panea, B., Olleta, J. L. and Sanudo, C. (2008). Near-infrared reflectance spectroscopy for predicting chemical, instrumental and sensory quality of beef. *Meat Sci.* **80**:697–702.

Rødbotten, R., Nilsen, B. N. and Hildrum, K. I. (2000). Prediction beef quality attributes from early post mortem near infrared reflectance spectra. *Food Chem.* **69**:427–436.

Roza-Delgado, B. de la, Soldado, A., Oliveira, A. F. G. de F., Martínez-Fernández, A. and Argamentería, A. (2014). Assessing the value of a portable near infrared spectroscopy sensor for predicting pork meat quality traits of "*Asturcelta* autochthonous swine breed". *Food Anal. Methods* **7**:151–156.

Sacchi, R., Medina, I., Aubourg, S. P., Addeo, F. and Paolillo, L. (1993). Proton nuclear magnetic resonance rapid and structure-specific determination of ω-3 polyunsaturated fatty acids in fish lipids. *JAOCS* **70** (3):225–228.

Sacchi, R., Medina, I., Paolillo, L. and Addeo, F. (1994). High-resolution ^{13}C-NMR olefinic spectra of DHA and acids, methyl esters and triacylglycerols. *Chem. Phys. Lipids* **69**:65–73.

Sadeghi-Jorabchi, H., Wilson, R. H., Belton, P. S., Ewards-Webb, J. D. and Coxon, D. T. (1991). Quantitative analysis of oils and fats by Fourier transform Raman spectroscopy. *Spectrochimica Acta A* **47**:1449–1458.

Sanderson, R., Lister, S. J., Dhanoa, M. S., Barnes, R. J. and Thomas, C. (1997). Use of near infrared reflectance spectroscopy to predict and compare the composition of carcass samples from young steers. *Animal Sci.* **65**:45–54.

Sanguansri, L. and Augustin, M. A. (2007). Microencapsulation and delivery of omega-3 fatty acids. in: Functional Food Ingredients and Nutraceuticals. Processing Technologies, pp. 297–327. Shi, J., (Ed.), CRC Press, Boca Raton, FL, USA.

Sato, T., Kawano, S. and Iwamoto, M. (1991). Near infrared spectral patterns of fatty acid analysis from fats and oils. *J. Am. Oil Chem. Soc.* **68** (11):827–833.

Savenije, B., Geesink, G. H., Van der Palen, J. G. P. and Hemke, G. (2006). Prediction of pork quality using visible/near-infrared reflectance spectroscopy. *Meat Sci.* **73**:181–184.

Schaare, P. N. and Fraser, D. G. (2000). Comparison of reflectance, interactance and transmission modes of visible-near infrared spectroscopy for measuring internal properties of kiwifruit (Actinidia chinensis). *Postharvest Biol. Technol.* **20**(2):175–184.

Schiavon, S., Tagliapietra, F., Dal Maso, M., Bailoni, L. and Bittante, G. (2010). Effect of low-protein diets and rumen-protected conjugated linoleic acid on production and carcass traits of growing double-muscled Piemontese bulls. *J. Anim. Sci.* **88**:3372–3383.

Segtnan, V. H., Høy, M., Lundby, F., Narum, B. and Wold, J. P. (2009). Fat distribution analysis in salmon using non-contact near infrared interactance imaging: a sampling and calibration strategy. *J. Near Infrared Spectrosc.* **17**:247–253.

Shackelford, S.D., Wheeler, T. L. and Koohmaraie, M. (1999). Tenderness classification of beef: II. Design and analysis of a system to measure beef longissimus shear force under commercial processing conditions. *J. Animal Sci.* **77**:1474–1481.

Shimamoto, J., Hiratsuka, S., Hasegawa, K., Sato, M. and Kawano, S. (2003). Rapid non-destructive determination of fat content in frozen skipjack using a portable near infrared spectrophotometer. *Fish. Sci.* **69**:856–860.

Shimamoto, J., Hasegawa, K., Sato, M. and Kawano, S. (2004). Non-destructive determination of fat content in frozen and thawed mackerel by near infrared spectroscopy. *Fisheries Sci.* **70**:345–347.

Sierra, V., Aldai, N., Castro, P., Osoro, K., Coto-Montes, A. and Olivan, M. (2008). Prediction of the fatty acid composition of beef by near infrared transmittance spectroscopy. *Meat Sci.* **78**:248–255.

Shingfield, K. J., Chilliard, Y., Toivonen, V., Kairenius, P. and Givens, D. D. (2008). Trans fatty acids and bioactive lipids in ruminant milk. *Adv. Exp. Med. Biol.* **606**:3–65.

Smith, E. and Dent, G. (2005). Modern Raman Spectroscopy, A Practical Approach. John Wiley & Sons Ltd, Chichester, West Sussex, England.

Solberg, C., Saugen, E., Swenson, L.-P., Bruun, L. and Isaksson, T. (2003). Determination of fat in live farmed Atlantic salmon using non-invasive NIR techniques. *J. Sci. Food Agric.* **83**:692–696.

Sollid, H. and Solberg, C. (1992). Salmon fat content estimation by near-infrared transmission spectroscopy. *J. Food Sci.* **57**:792–793.

Sørensen, K. M., Petersen, H. and Engelsen, S. B. (2012). An on-line near-infrared (NIR) transmission method for determining depth profiles of fatty acid composition and iodine value in porcine adipose fat tissue. *Appl. Spectrosc.* **66**(2):218–226.

Sørland, G. H., Larsen, P. M., Lundby, F., Rudi, A.-P. and Guiheneuf, T. (2004). Determination of total fat and moisture content in meat using low field NMR. *Meat Sci.* **66**:543–550.

Standal, I. B., Axelson, D. E. and Aursand, M. (2009). Differentiation of fish oils according to species by ^{13}C-NMR regiospecific analyses of triacyglycerols. *J. Am. Oil Chem. Soc.* **86**:401–407.

Stark, A. H., Crawford, M. A. and Reifen, R. (2008). Update on α-linolenic acid. *Nutrition Rev.* **66**:326–332.

Stone, N. J. (1996). Fish consumption, fish oil, lipids, and coronary heart disease. *Circulation* **94**(9):2337–2340.

Su, H., Sha, K., Zhang, L., Zhang, Q., Xu, Y., Zhang, R., Li, H. and Sun, B. (2014). Development of near infrared reflectance spectroscopy to predict chemical composition with a wide range of variability in beef. *Meat Sci.* **98** (2):110–114.

Suárez, E. R., Mugford, P. F., Rolle, A. J., Burton, I. W., Walter, J. A. and Kralovec, J. A. (2010). ^{13}C-NMR regioisomeric analysis of EPA and DHA in fish oil derived triacylglycerol concentrates. *J. Am. Oil Chem. Soc.* **87**:1425–1433.

Tengku-Rozaina, T. M. and Birch, E. J. (2014). Positional distribution of fatty acids on hoki and tuna oil triglycerides by pancreatic lipase and ^{13}C NMR analysis. *Eur. J. Lipid Sci. Technol.* **116**:272–281.

Thompson, J. (2004). The effects of marbling on flavour and juiciness scores of cooked beef, after adjusting to a constant tenderness. *Anim. Prod. Sci.* **44**(7):645–652.

Tingle, J. M., Pope, J. M., Baumgartner, P. A. and Sarafis, V. (1995). Magnetic resonance imaging of fat and muscle distribution in meat. *Int J. Food Sci. Technol.* **30**:437–446.

Tøgersen, G., Isaksson, T., Nielsen, B. N., Baker, E. A. and Hildrum, K. I. (1999). On-line NIR analysis of fat, water and protein in industrial scale ground meat batches. *Meat Sci.* **51**:97–102.

Tøgersen, G., Arnesen, J. F., Nielsen, B. N. and Hildrum, K. I. (2003). On-line prediction of chemical composition of semi-frozen ground beef by non-invasive NIR spectroscopy. *Meat Sci.* **63**:515–523.

Toussaint, C. A., Médale, F., Davenel, A., Fauconneau, B., Haffray, P. and Akoka, S. (2002). Determination of the lipid content in fish muscle by a self-calibrated NMR relaxometry method: Comparison with classical chemical extraction methods. *J. Sci. Food Agric.* **82** (2):173–178.

Valdes, E. V., Atkinson, J. L., Hilton, J. W. and Leeson, S. (1989). Near infrared reflectance analysis of fat, protein and gross energy of chicken and rainbow trout carcass. *Canadian J. Animal Sci.* **69**:1087–1090.

Vanschoonbeek, K., de Maat, M. P. M. and Heemskerk, J. W. M. (2003). Fish oil consumption and reduction of arterial disease. *J. Nutr.* **133**:657–660.

Veliyulin, E., van der Zwaag, C., Burk, W. and Erikson, U. (2005). In vivo determination of fat content in Atlantic salmon (Salmo salar) with a mobile NMR spectrometer. *J. Sci. Food Agric.* **85**:1299–1304.

Viljoen, M., Hoffman, L. C. and Brand, T. S. (2007). Prediction of the chemical composition of mutton with near infrared reflectance spectroscopy. *Small Ruminant Res.* **69**:88–94.

Vote, D. J., Belk, K. E., Tatum, J. D., Scanga, J. A. and Smith, G. C. (2003). Online prediction of beef tenderness using a computer vision system equipped with a BeefCam module. *J. Animal Sci.* **81**:457–465.

Wheeler, T., Cundiff, L. and Koch, R. (1994). Effect of marbling degree on beef palatability in Bos taurus and Bos indicus cattle. *J. Anim. Sci.* **72** (12):3145–3151.

Williams, P. and Norris, K.. (1987). Near-infrared technology in the agricultural and food industries: American Association of Cereal Chemists, Inc.

Windham, W. R., Lawrence, K. C. and Feldner, P. W. (2003). Prediction of fat content in poultry meat by near-infrared transmission analysis. *J. Appl. Poultry Res.* **12**:69–73.

Wold, J. P., Jakobsen, T. and Krane, L. (1996). Atlantic salmon average fat content estimated by near-infrared transmittance spectroscopy. *J. Food Sci.* **61**(1):74–77.

Wold, J. P. and Isaksson, T. (1997). Non-destructive determination of fat and moisture in whole atlantic salmon by near-infrared diffuse spectroscopy. *J. Food Sci.* **62**(4):734–736.

Wold, J. P., Marquardt, B. J., Dable, B. K., Robb, D. and Hatlen, B. (2004). Rapid quantification of carotenoids and fat in Atlantic Salmon (Salmo salar L.) by Raman spectroscopy and chemometrics. *Appl. Spectrosc.* **58**(4):395–403.

Wold, J. P., O'Farrell, M., Høy, M. and Tschudi, J. (2011). On-line determination and control of fat content in batches of beef trimmings by NIR imaging spectroscopy. *Meat Sci.* **89**:317–324.

Wood, J. D., Enser, M., Fisher, A. V., Nute, G. R., Richardson, R. I. and Sheard, P. R. (1999). Manipulating meat quality and composition. *The Proceedings of the Nutrition Society* **58**:363–370.

Wood, J. D., Richardson, R. I., Nute, G. R., Fisher, A. V., Campo, M. M., Kasapidou, E., Sheard, P. R. and Enser, M. (2004). Effects of fatty acids on meat quality: A review. *Meat Sci.* **66**:21–32.

Wood, J. D., Enser, M., Fisher, A. V., Nute, G. R., Sheard, P. R., Richardson, R. I., Hughes, S. I., Whittington, F. M. (2008). Fat deposition, fatty acid composition and meat quality: A review. *Meat Sci.* **78**:343–358.

Wu, D., Chen, X., Cao, F., Sun, D.-W., He, Y. and Jiang, Y. (2014). Comparison of infrared spectroscopy and nuclear magnetic resonance techniques in tandem with multivariable selection for rapid determination of ω-3 polyunsaturated fatty acids in fish Oil. *Food Bioprocess Technol.* **7**:1555–1569.

Wu, D. and Sun, D.-W. (2013). Advanced applications of hyperspectral imaging technology for food quality and safety analysis and assessment: A review-Part I: Fundamentals. *Innov. Food Sci. Emerg. Technol.* **19**:1–14.

Zamora-Rojas, E., Garrido-Varo, A., Pedro-Sanz, E. D., Guerrero-Ginel, J. E. and Pérez-Marín, D. (2011). Monitoring NIRS calibrations for use in routine meat analysis as part of Iberian pig-breeding programs. *Food Chem.* **129**:1889–1897.

Zhang, H.-Z. and Lee, T.-C. (1997). Rapid near-infrared spectroscopic method for the determination of free fatty acid in fish and its application in fish quality assessment. *J. Agric. Food Chem.* **45**:3515–3521.

Zhang, J., Sasaki, S., Amano, K. and Kesteloot, H. (1999). Fish consumption and mortality from all causes, ischemic heart disease, and stroke: an ecological study. *Prev. Med.* **28**(5):520–529.

Zhou, L. J., Wu, H., Li, J. T., Wang, Z. Y. and Zhang, L. Y. (2012). Determination of fatty acids in broiler breast meat by near-infrared reflectance spectroscopy. *Meat Sci.* **90**:658–664.

Zhu, F., Zhang, H., Shao, Y., He, Y. and Ngadi, M. (2014). Mapping of fat and moisture distribution in Atlantic salmon using near-infrared hyperspectral imaging. *Food Bioprocess Technol.* **7**(4):1208–1214.